NATIONAL ADVISORY COMMITTEE FOR AERONAUTICS

TECHNICAL NOTE 2991

ACCELERATIONS AND PASSENGER HARNESS LOADS MEASURED IN FULL-SCALE LIGHT-AIRPLANE CRASHES

By A. Martin Eiband, Scott H. Simpkinson
and Dugald O. Black

Lewis Flight Propulsion Laboratory
Cleveland, Ohio

Washington
August 1953

ERRATA No. 1

NACA TN 2991

ACCELERATIONS AND PASSENGER HARNESS LOADS MEASURED IN FULL-SCALE LIGHT-AIRPLANE CRASHES

By A. Martin Eiband, Scott H. Simpkinson
and Dugald O. Black

August 1953

Page 22, box heading of fifth column should read as follows:
Total duration of major peaks of longitudinal deceleration of fuselage at rear seat, sec.

NATIONAL ADVISORY COMMITTEE FOR AERONAUTICS

TECHNICAL NOTE 2991

ACCELERATIONS AND PASSENGER HARNESS LOADS MEASURED IN FULL-SCALE LIGHT-AIRPLANE CRASHES

By A. Martin Eiband, Scott H. Simpkinson,
and Dugald O. Black

SUMMARY

Full-scale light-airplane crashes simulating stall-spin accidents were conducted to determine the decelerations to which occupants are exposed and the resulting harness forces encountered in this type of accident. Crashes at impact speeds from 42 to 60 miles per hour were studied. The airplanes used were of the familiar steel-tube, fabric-covered, tandem, two-seat type.

In crashes up to an impact speed of 60 miles per hour, crumpling of the forward fuselage structure prevented the maximum deceleration at the rear-seat location from exceeding 26 to 33g. This maximum g value appeared independent of the impact speed. Restraining forces in the seat-belt - shoulder-harness combination reached 5800 pounds. The rear-seat occupant can survive crashes of the type studied at impact speeds up to 60 miles per hour, if body movement is restrained by an adequate seat-belt - shoulder-harness combination so as to prevent injurious contact with obstacles normally present in the cabin. Inwardly collapsing cabin structure, however, is a potential hazard in the higher-speed crashes.

INTRODUCTION

Light-airplane accident data, compiled by Crash Injury Research of Cornell University Medical College, indicate that human beings have often withstood decelerations in excess of those imposed in airplane crashes involving extensive damage to the airplane structure (ref. 1). This study also correlates the extent of damage to the airplane structure with the injury incurred by the occupants during crash accidents. The Cornell work indicates that the stall-spin is a common light-airplane accident configuration. In this type of crash, fatalities often occur; but the passenger in the rear seat frequently survives when adequately restrained. Collapse of the front portion of the cabin is often fatal to the front passenger. However, the magnitudes of acceleration to which the occupants were subjected during these accidents were unknown.

The NACA Lewis laboratory has studied the accelerations resulting from simulated stall-spin accidents at impact speeds of 42, 47, and 60 miles per hour. In these studies, dummy passengers were installed in small two-seat, tandem airplanes (fig. 1(a)), and a record was obtained of the accelerations transmitted through the airplane structure to the rear-seat occupant during the crash. The accelerations and the harness forces recorded on the dummy were related to the events in the crash sequence by comparing them with the crash action recorded on motion-picture film. The data obtained in these crashes are intended as a contribution to the general background of engineering information required for the design of improved seats and harnesses for greater crash safety.

APPARATUS AND PROCEDURE

Type of Crash Simulated

The light-airplane crashes were designed to simulate accidents in which the airplane stalls and strikes the ground just as it enters a spin. An inspection of stall-spin accident records indicates that generally the left wing tip, the left landing-gear wheel, and the engine of the airplane strike the ground simultaneously. To simulate such a crash, the airplane was made to strike an earthen crash barrier as shown in figure 1(a). The barrier in this arrangement corresponds to the ground in an actual crash.

In these tests, the approach to the crash barrier was made in a horizontal direction instead of a nearly vertical direction as would be the case in a real accident; therefore, the forces in the direction of motion are in error by a factor of approximately 1 unit of gravity. This error in forces is small in comparison with the forces measured in the crash.

Operating Technique

In a crash, the airplane was propelled by its own power along a guide rail toward the crash barrier. A slipper, located at the end of a tongue, guided the airplane to the crash barrier. This guide slipper was designed to fit around the top flange of the guide rail (fig. 1(b)) in such a manner as to prevent the slipper from leaving the rail in either a vertical or a lateral direction. In order to prevent the slipper and tongue assembly from transmitting forces to the airplane structure during the crash, a 12-inch-diameter steel tube (fig. 1(c)) was installed at the end of the rail to allow the slipper and the tongue assembly to pass underneath the crash barrier. The momentum of the slipper and tongue assembly carried it into the steel tube upon airplane impact with the crash barrier. The rear of the tongue was pinned to the airplane with a 3/32-inch-diameter pin (fig. 1(d)) that sheared under a load of 150 pounds.

In order to support the airplane in flight attitude as it proceeded unmanned down the runway, a tail truss was bolted to the tail-wheel attachment bracket (fig. 1(e)), the tail-wheel assembly having been removed. A 1/8-inch aluminum plate that was flush-riveted to the bottom of the tail truss slid along on top of the guide rail. This tail truss weighed approximately $2\frac{1}{2}$ pounds more than the tail-wheel assembly that it replaced. The gross weight of each airplane was 1200, 1013, and 1261 pounds, respectively, for the crashes at 42, 47, and 60 mph. The Civil Aeronautics Administration certified maximum weight of the airplane is 1220 pounds.

An anchor pier (fig. 1(f)) was installed on the guide rail at the rear of the airplane to retain the airplane under take-off power without brakes. A tensiometer measured the static thrust of the airplane just before being released.

The earthen crash barrier (fig. 1(a)) located at the end of the guide rail was constructed of dirt compacted to have a bearing pressure of 5900 pounds per square foot on the front surface into which the airplane crashed. This bearing pressure corresponds to the local undisturbed clay turf soil. The barrier was 50 feet long, $9\frac{1}{2}$ feet high, and 22 feet thick at the base, sloped at an angle of 55° to the vertical axis, and oriented 66° to the axis of the rail, as shown in the sketch in figure 2.

The dummy in the front seat (fig. 3) was a standard Air Force dummy designed for use in the testing of parachutes. This dummy had a skeleton of steel members pinned at the joints with bolts. The skeleton was covered with felt padding, and the skin was made of a heavy canvas cloth. No attempt was made in the construction of the dummy to simulate the rigidity of the human body, although the mass distribution of the component parts of the dummy was similar to that of a human being. This dummy was held in the seat by a standard 2-inch seat belt attached to the front seat of the airplane.

The Air Force anthropomorphic dummy was installed in the rear seat of the airplane as shown in figure 3. This dummy was designed by the Wright Air Development Center Aero Medical Laboratory. The dummy skeleton was made of steel, and some members were made to simulate the strength of those of the human body. Elastic shock cords were used to simulate muscles or tendons, and sponge rubber was used for the flesh and skin. This dummy was a reasonable replica of the human body in both mass distribution and resilience of human tissue. However, the reaction of the dummy to deceleration differed from the human body because of the absence of muscular reflex action. The seat belt and the shoulder harness used to restrain this dummy were attached to the basic structure of the airplane.

The airplane configuration and the dummy installation for each of the three impact crashes are given in the following table:

Impact speed, mph	Seat location	Type of dummy	Restraining harness	Airplane fuel-tank contents
60	Front	Parachute	2-inch seat belt	72 lb water (dyed red)
	Rear	Anthropomorphic	1. Shoulder harness 2. 3-inch seat belt	
47	Front seat removed			Empty
	Rear	Anthropomorphic	2-inch and 3-inch seat-belt combination	
42	Front	Parachute	2-inch seat belt	Empty
	Rear	Anthropomorphic	1. Shoulder harness 2. 3-inch seat belt	

INSTRUMENTATION

Accelerometers

Accelerations of the head and the chest of the anthropomorphic dummy installed in the rear seat of the airplane were obtained from telemetered accelerometer data. Accelerometers also were used to measure the accelerations on the airplane structure at the rear seat. Measurement of the forces exerted by the dummy on the seat belt and shoulder harness was made by tensiometers installed at each attachment point of the restraining harness.

Three accelerometers, attached to the fuselage-floor structure at the rear seat, measured accelerations along the longitudinal, vertical, and lateral axes of the airplane. Three accelerometers, installed on the chest of the anthropomorphic dummy, measured accelerations (1) longitudinally (perpendicular to the spine in the fore and aft plane), (2) vertically (parallel to the spine), and (3) laterally (left and right). One accelerometer was installed in the head of the anthropomorphic dummy to measure accelerations perpendicular to the face.

Tensiometers

Tensiometers were installed at each end of the seat belt and at the anchor point on the shoulder harness of the anthropomorphic dummy to measure the forces exerted on the restraining harness by the dummy throughout the crash.

Telemeter System

A simple telemeter system that was readily available afforded a convenient method for obtaining continuous records throughout the crash of the accelerations and the harness forces. The telemeter transmitter was located in the airplane as shown in figure 4(b). The receiving and recording station, as located in the operations building (ref. 2), is shown in figure 4(c).

Two types of transducer were used in the telemeter configuration. The accelerometers were of the variable-inductance, suspended-slug type (fig. 4(d)) and were designed to have a linear change in inductance from -90 to 90g in the sensitive direction and to have at least a 100:1 attenuation of response in the two nonsensitive directions. The tensiometers were also in the variable-inductance category of transducers. They consisted of two rigidly interconnected beams that spaced a powdered iron slug within a coil (fig. 4(d)). Tension applied by the seat belt or shoulder harness caused the beams to deflect, resulting in a relative displacement between the slug and coil and thereby producing a change in the apparent inductance at the terminals. Location of instrumentation is given in the following table:

Channel	Measured quantity	Direction	Location	Figure	Range
1	Acceleration	Longitudinal	Chest of dummy	4(e)	-88 to 38g
2	Acceleration	Vertical	Chest of dummy	4(e)	-91 to 42g
3	Acceleration	Lateral	Chest of dummy	4(e)	-65 to 66g
4	Acceleration	Longitudinal	Fuselage floor at rear seat	4(g)	-91 to 38g
5	Acceleration	Vertical	Fuselage floor at rear seat	4(g)	-81 to 32g
6	Acceleration	Lateral	Fuselage floor at rear seat	4(g)	-50 to 50g
7	Tension	----------	Shoulder harness of rear dummy	4(h)	0 to 5000 lb
8	Acceleration	Longitudinal	Head of rear dummy	4(f)	-43 to 45g
9	Tension	----------	Seat belt, left side of rear dummy	4(i)	0 to 4800 lb
10	Tension	----------	Seat belt, right side of rear dummy	4(i)	0 to 5000 lb

Figure 4(a) shows the general location of the instrumentation in the airplane. The ten channels available in the telemeter system were used to measure the quantities listed in the preceding table. Figures 4(e) to (i), listed in the table, show the specific location of each transducer as installed on the dummy or in the airplane.

The transmitting station and batteries were protected by two aluminum boxes, one installed inside the other. The inner box, to which the station and batteries were rigidly mounted, was suspended on all sides by corrugated pasteboard as shown in figure 4(b). The outside aluminum box was supported in the airplane by a mount built up of welded tubing. This unit is shown before and after installation in the airplane in figure 4(b). The construction was designed to limit the expected short-duration, high-peak accelerations imposed on the transmitting station. The separate units of this transmitting station were previously checked along the three major axes on a spin-type g-table and on a vibrating table at values up to 25g from 0 to 200 cycles per second with less than 1/2 percent of full-scale change in the transmitted data. (This is not an indication of flat response to 200 cps, as the accelerometers were not on the shake tables; this test was strictly an equipment survival check.) In the 47-mph crash, a channel was left vacant. The subcarrier oscillator for this channel was tuned with a fixed inductance to the center frequency of the channel and allowed to operate through the crash. The oscillograph records of the ten channels of telemetered data from the 47-mph crash are shown in figure 4(j). The record of fixed channel 7 clearly shows that the accelerations carried through to the equipment section had no effect on the data.

The telemeter system, exclusive of transducers and recorders, according to statistical unpublished data has an accuracy of ±2 percent of full-scale amplitude and a frequency response of flat within ±2 percent from steady-state conditions to 200 cps. The nature of FM discriminators is such that an increase in amplitude lowers the limit of flat frequency response; and in this case it must be stated that for steady-state levels the full-scale amplitude was faithfully reproduced, while at 200 cps the amplitude had to be held within ±20 percent of full scale from the center of the range in order to have within ±2 percent flat frequency response. The data in this report are within this region with the exception of the case in which the rear dummy's head hit the neck of the forward dummy in the 60-mph crash. The accelerometers had a measured undamped natural frequency of approximately 300 cps. They were filled with 2400-centistoke silicone damping fluid and individually checked for a damping ratio of 0.60 to 0.64. This damping ratio resulted in flat response within 5 percent, up to 85 percent of the undamped natural frequency. Thus the accelerometer response was flat within 5 percent to 250 cps. The seat-belt and shoulder-harness tensiometers had a calculated undamped natural frequency (first mode) of 1920 cps; and, since an undamped system has a flat response within 5 percent up to 22 percent of the undamped natural frequency, this system did not require any damping, being flat within 5 percent up to 420 cps.

The frequency responses of the recording galvanometers used in the 60-mph crash were chosen with a specific measurement in mind and were as follows: Galvanometers which had a response that was flat within 5 percent to 300 cps were used for recording the three components of acceleration of the rear dummy's chest and of the floor under the rear seat and the acceleration in the top of the dummy's head. The galvanometers used to record the belt tensions were flat within 5 percent to 180 cps. An inspection of the telemeter records revealed that the basic data were relatively low in frequency, except for the accelerations on the floor, and the response of the system was well over that required. The high-frequency response of the galvanometers, however, did produce records that were hard to read because of the intermodulation present. In this crash, bursts of noise occurred simultaneously in all the recorded channels throughout the run and almost obliterated the crash record. By taxi tests on an airplane the source of this noise was determined to be unbonded metal parts chaffing together. This problem was overcome by using short heavy ground straps around all metallic links, and by covering the control cables with plastic tubing to prevent intermittent grounding to adjacent metal (fig. 4(k)). In order to produce cleaner, easier-to-read records, without impairing the accuracy of the data, the galvanometers used to record the chest accelerations and belt tensions were changed in the 42- and 47-mph crashes to a type having a frequency response of flat within 5 percent to 100 cps.

Airplane Velocity

The ground speed of the airplane was determined by electronic timers as described in reference 2. In addition, the ground speed was determined by time-displacement studies of high-speed motion pictures.

Motion-Picture Cameras

Motion-picture cameras located on the various camera platforms around the crash barrier recorded the destruction of the airplane at the barrier, the area of fuel spillage, and the motion of the dummies installed in the fuselage.

Mitchell, Ciné, Fastax, and K-24 cameras, all operating electrically within the range of film speeds shown in reference 2, were used in each crash. The locations of the camera stations are shown in figure 2.

Because the natural illumination of the cabin area in the first crash was insufficient to record clearly the action of the dummies, additional light was provided for subsequent crashes. This light source comprised a bank of 96 tungsten, focal-plane, flash bulbs (fig. 4(l)). These bulbs were set off in sets of four distributed along the decelerating distance of the airplane. Twenty-four sets of four flash bulbs produced peak illumination for a duration of 1 second.

Calculated Acceleration Curves

Curves of longitudinal deceleration of the engine in all three crashes and of the fuselage floor under the rear seat in the 60-mph crash were calculated from the photographic time-displacement data with equal time increments of 0.005 second. Calculation of engine deceleration was necessary, since no accelerometers were installed on the engine because of the limited number of telemetering channels available. Longitudinal fuselage deceleration during the 60-mph crash was calculated, because the accelerometer data in this crash were rendered invalid by structural failure of the members on which the accelerometers were mounted.

Definition of Accelerations

Since the accelerations along the longitudinal, vertical, and lateral axes are to be considered, it is necessary to designate a direction for each.

The sketches in figure 5 of seated dummies show clearly the direction and define the linear accelerations along the longitudinal and vertical axes. Accelerations along the longitudinal axis of the airplane that increase the forward speed of the airplane are positive (+g) as shown in figure 5(a). When the airplane experiences positive acceleration in the longitudinal direction, the dummy's back presses against the seat back. In a negative acceleration in the longitudinal direction, the dummy moves forward with respect to the seat and is restrained by the seat belt and shoulder harness as shown in figure 5(b). To simplify language, "deceleration" will be used in place of negative longitudinal acceleration (-g). Accelerations along the vertical axis in which the dummy is thrust upward are called "positive accelerations" (+g) as shown in figure 5(c). Accelerations in which the body is pulled downward by the shoulder harness and seat belt (fig. 5(d)) are called "negative accelerations" (-g). Left or right lateral accelerations produce a respective displacement of the dummy to the left or the right from the neutral position.

RESULTS AND DISCUSSION

Acceleration Along Longitudinal Axis of Airplane

60-Mph crash. - In this section a comparison is made of the longitudinal acceleration of the fuselage at the rear seat with respect to the engine, and the acceleration experienced by the rear dummy's chest and head in response to the airplane accelerations. The shoulder-harness and seat-belt forces associated with these accelerations are also discussed.

In figure 6(a) the acceleration of the airplane structure and of the dummy are compared for the crash in which the airplane speed was 60 mph upon impact with the barrier. Time is counted from the moment the airplane propeller tip strikes the barrier. The deceleration on the engine (fig. 6(a)) rises rapidly at a rate of 4130g per second to a peak value of 62g and remains at this value for 0.015 second. The deceleration of the fuselage is attenuated by the crumpling of the structure between the engine and the fuselage floor at the rear-seat position. This crumpling reduces the rate of onset of deceleration from 4130g per second on the engine to 1500g per second on the floor and also reduces the magnitude of this deceleration. Four peak values of deceleration occur on the fuselage floor. These peaks vary from 25 to 33g and occur at time intervals of approximately 0.023 second.

A delay of 0.023 second between the onset of fuselage floor deceleration and the onset of chest deceleration is believed to be the forward movement of the chest of the dummy of approximately 2 inches relative to the seat. This relative forward movement of the chest is an accumulation of displacement partly due to (1) slack in all components of the restraining harness, (2) elongation of the harness under the initial load, and (3) the resilience of the sponge-rubber flesh of the abdominal, thoracic, and shoulder regions of the dummy. The resulting overshooting of peak values of the chest deceleration, when compared with the deceleration of the fuselage floor, is then dependent upon the mass-spring characteristics of the dummy and its restraining mechanism. The magnitude of the first peak of chest deceleration of 34g thus exceeded the first peak value of fuselage floor deceleration of 25g by 28 percent. A maximum chest deceleration of 50g was obtained at 0.118 second after impact.

After the slack in the seat belt and shoulder harness is taken up by the beginning of deceleration of the dummy, the dummy, the restraining belts, and the airplane structure begin to respond to the decelerative force applied at the nose of the airplane as components of an interdependent elastic system. Because the mass of the dummy is comparable to that of the fuselage, the fuselage floor deceleration may be directly affected by the load imposed on the airplane structure by the dummy. Thus, once the rear dummy reaches its first peak of deceleration at 0.073 second following impact, the fuselage floor deceleration responds in some measure to the change in loading on the airplane structure imposed by the deceleration of the dummy. Since the gross airplane weight was 1260 pounds, the weight of the rear dummy approximately 200 pounds and that of the front dummy 155 pounds, the interrelation of the deceleration history of the dummies with that of the fuselage under the rear seat during the crash is apparent. Following the first peak in fuselage deceleration (fig. 6(a)), this interrelation appears as each peak in fuselage floor deceleration occurs at approximately 0.01 second after the corresponding peak in dummy deceleration. The last marked peak value in floor deceleration follows the last peak value in dummy deceleration by 0.007 second.

Head deceleration in the 60-mph crash began at 0.062 second after impact, following a delay of 0.01 second after the beginning of chest deceleration. Head deceleration did not reach appreciable magnitudes until 0.10 second after impact. The delay in the build-up of head deceleration was due to movement of the head relative to the chest up to 0.10 second after impact. The rise in head deceleration between 0.10 and 0.11 second indicates contact of the chin with the chest. This contact was observed in the motion-picture film at about 0.10 second after impact.

The sharp rise in deceleration that began at 0.11 second indicates contact of the rear dummy's helmet with the steel neck-joint of the front dummy. The manner in which the helmet contacted the neck joint of the front dummy was established in the post-crash analysis. The inset in figure 6(a) shows a post-crash reconstruction of this contact. Two peaks of over 100g deceleration were recorded, but, since the response of the instrument for such sharp rises was not flat for values above 55g, any values above this amount are subject to unpredictable error.

47-Mph crash. - Similar engine-fuselage-chest-head data for the 47-mph crash are presented in figure 6(b). The peak engine deceleration in the 47-mph crash reached 46g in 0.041 second after impact, then dropped to a plateau of 31g. The engine deceleration exceeded 31g for 0.016 second. Crumpling of the airplane structure is responsible for the decline of the maximum deceleration of 46g at the engine to 32.5g at the fuselage floor. Four peak values of deceleration occur on the fuselage floor and vary from 32.5 to 27.5g for approximately 0.38 second. As shown by figure 6(b), onset of dummy chest deceleration lagged onset of engine deceleration by about 0.01 second. The rate of increase of chest deceleration of 980g per second was appreciably reduced from 4600g per second at the engine and 4300g per second at the fuselage. Maximum chest deceleration of the dummy reached 46g by 0.088 second after impact.

Head deceleration of low magnitude persisted until 0.122 second after impact. The rapid increase in head deceleration, beginning at 0.122 second, occurred after the head had broken loose from the shoulders. Observation of the motion-picture data definitely established failure of the neck by 0.121 second. [Failure of the neck of this dummy is in no way indicative of the probability of decapitation of a human being, as humans have repeatedly survived decelerations up to 45g with no indication of neck injury (ref. 3).]

42-Mph crash. - Data for the 42-mph crash are presented in figure 6(c). The maximum engine deceleration was 32g with a duration of deceleration in excess of 30g existing for 0.016 second. Reduction in the rate of onset of fuselage deceleration from that of the engine was not as pronounced in the lower-speed crashes as it was in the 60-mph crash. The maximum engine deceleration of 30 to 32g was reduced to 26g at the fuselage-floor position. Maximum peak deceleration of the dummy's chest reached 32.5g by 0.084 second after impact. A second peak chest deceleration of 26.5g occurred at 0.125 second after impact.

No appreciable deceleration of the rear dummy's head in the 42-mph crash was recorded until after the head was detached at 0.096 second, in a manner similar to that of the 47-mph crash.

In the record of fuselage-floor deceleration during the 60-mph crash, constant velocity is indicated up to the time of onset of engine deceleration. During the corresponding time in the 47- and 42-mph crashes, however, alternate fluctuations of positive and negative acceleration were recorded (figs. 6(b) and (c)). The highest of these frequencies is approximately 100 cps. These fluctuations of longitudinal acceleration of the fuselage floor probably are associated with the facts that the guide slipper leaves the end of the guide rail, the propeller tips contact the barrier, and the guide slipper strikes the bottom of the tunnel before the guide tongue is completely detached from the airplane. The absence of any indicated change in fuselage velocity in the 60-mph crash is due to the relative accuracy with which changes in the rate of displacement of the engine could be recorded by photographic data, compared with that of the accelerometer-telemeter system.

Effect of Impact Speed on Longitudinal Deceleration

Fuselage. - The effect of impact speed on the longitudinal deceleration of the fuselage floor at the rear seat is shown in figure 7. These data indicate that the maximum deceleration does not change appreciably with impact speed. The maximum g for the three crashes varied from 26.5 to 33.5g. This small change in peak deceleration indicates that the structure will sustain only a certain force before a section begins to fail. As each section fails, the load shifts to other sections, until the total decelerative force has been reduced below the magnitude that causes failure of the structure.

In the 60-mph crash, the fuselage crumpled to such a degree as to allow the leading edge of the wings to come in contact with the crash barrier, and the resulting damage to the wing structure is shown in figure 8(a). This impact of the wings with the barrier undoubtedly aided in reducing the decelerative force that was transmitted to the fuselage because part of the mass of the wings was decelerated by direct

contact with the barrier. Very little damage occurred to the wings in the 47- and 42-mph crashes, as shown in figures 8(b) and (c). Since the maximum fuselage-floor deceleration for the three crashes did not vary appreciably, the duration of the decelerations increased with increasing impact speed consistently with the higher airplane momentum at impact. A measure of this duration can be obtained by noting the time of the last major peak (fig. 7). This peak for the 60-mph crash occurred at 0.124 second after impact. The last peak deceleration for the 47-mph crash occurred at 0.076 second after impact, and the last peak for the 42-mph crash occurred at 0.061 second after impact. The average rate of onset of deceleration of the fuselage floor for the 42- and 47-mph crashes was approximately 2400g per second and 4600g per second, respectively.

Chest of dummy. - In making a comparison of the chest decelerations to determine the effect of impact speed, data from the 47-mph crash were deleted, because the dummy was installed with only seat-belt restraint. The absence of a shoulder harness permitted the torso to flex around the seat belt. Figure 9 is a plot of the longitudinal deceleration of the chest against time for the 42- and the 60-mph crashes. Decreasing the impact speed from 60 to 42 mph reduced the number of major deceleration peaks from three to two and also reduced the magnitude of the largest deceleration peak from 50 to 32g. The general over-all time during which the deceleration was applied for the two impact speeds was approximately the same. The rate of onset of deceleration decreased from 2200g per second for the 60-mph crash to 950g per second for the 42-mph crash.

The peak deceleration for the chest increased slightly more than linearly with impact speed, whereas the peak deceleration for the fuselage was not appreciably affected by impact speed. The total time during which major chest deceleration occurred did not change appreciably with impact speed (fig. 9), but the total time during which the major peaks of fuselage deceleration occurred varied from 0.023 second for the 42-mph crash to 0.070 second for the 60-mph crash (fig. 7).

Lateral Accelerations

The lateral accelerations in figure 10 were recorded during the crash at an impact speed of 42 mph. As indicated in figure 10, these accelerations are insignificant relative to the magnitudes of the accelerations transmitted longitudinally and vertically from the fuselage to the dummy. Lateral acceleration of the dummy's chest and the fuselage floor reached peak values of 5 and 6g, respectively, whereas vertical and longitudinal acceleration of the dummy's chest reached 18 and 32g, respectively (fig. 11(a)). Vertical and longitudinal

fuselage-floor acceleration reached respective peaks of 9 (fig. 12) and 26g (fig. 6(c)). While peak values of lateral acceleration recorded on the dummy's chest were approximately the same as those recorded on the fuselage floor, there appears to be no phase correlation between the two records. Despite the asymmetrical crash configuration, the lateral accelerations do not indicate any tendency to predominate in either direction. The general trends in lateral acceleration existing in the 42-mph crash are also found in the 47- and 60-mph crashes.

Restraining Forces

Preliminary static tests of safety-harness components. - Several types of airplane seat belt and shoulder harness were tensile-tested statically to determine their breaking and elongation characteristics before being installed on the Air Force anthropomorphic and standard parachute dummies for the light-airplane crashes. Composite photographs of the seat belt and shoulder harness, the stress and strain curves, and the specifications of each harness are shown in figure 13. All static belt tests, except the test shown in figure 13(b), were conducted by installing the belts in a tensile machine so that a straight pull was induced lengthwise along the belts. Static tests of the 2-inch wide, commerical seat-belt assembly (fig. 13(a)) resulted in an elongation of $7\frac{1}{2}$ inches under a 1515-pound tensile load before failure occurred. The webbing failed because of the cutting action of the serrations of the buckle clamp.

Other investigators (ref. 4) have considered the possibility that in a crash, contrary to the generally used static test configuration, the load on the seat belt is so applied that the stresses in the belt fibers are unequal. This unequal stress distribution is caused by flexion of the torso over the seat belt in the pelvic region in such a manner that the two edges are folded toward each other. For the purpose of comparing such an asymmetrical loading with a straight-pull tensile test, a 2-inch seat belt was tested in a tensile machine with the test fixture shown in figure 13(b). This fixture held the belt in a simulated crash configuration that included curvature of the pelvic region, folding together of the belt edges across the pelvic region, and a total belt length comparable to that used in the straight-pull static test.

In this static test, using the test fixture, the seat belt failed at 3020 pounds total load after a total elongation of $8\frac{5}{8}$ inches. Failure of the belt was caused by the cutting action of the buckle as indicated

in figure 13(b). Comparison of the breaking load of the belt under the asymmetrical loading with the straight-pull loading indicated that fiber stresses during the static testing are of the same order, about 1500 pounds. Thus, no unequal fiber stresses are indicated in the asymmetrical loading during static testing. For this reason, the seat-belt loads recorded in the crash employing the 2-inch seat belt are comparable with either of the values found from the tensile tests.

The 3-inch military seat-belt assembly (fig. 13(c)) was tensile-tested in a straight pull. It failed under a load of 2620 pounds after stretching a total of $5\frac{1}{8}$ inches. Failure of this belt assembly was caused by cutting of the webbing by the adjusting buckle. In removing this belt assembly from the tensile machine the hook of the fastening buckle was found to be broken (fig. 13(c) inset). This break was not observed during the test; therefore, the load at which the hook of the buckle failed is not known.

The military shoulder-harness assembly (fig. 13(d)) was tensile-tested to failure. This failure occurred because of the cutting action of the adjusting buckle on the webbing. Prior to failure of the webbing, approximately 2 inches of the stitching at the junction of the two individual shoulder straps failed. This belt assembly failed under a load of 4725 pounds with a total elongation of $13\frac{1}{4}$ inches (fig. 13(d)).

Restraining Forces During Crash

42-Mph crash. - The forces acting through the seat belt and the shoulder harness to restrain the dummy in his seat and the accelerations applied to the chest of the dummy in the 42-mph crash are shown in figure 11(a) and (b). Vertical and longitudinal chest accelerations are plotted in figure 11(a). Total seat-belt force, plotted in figure 11(b) with longitudinal chest deceleration and shoulder-harness force, is the sum of the forces recorded at each end of the seat belt.

During the first 0.04 second following the onset of longitudinal chest deceleration, the seat-belt and shoulder-harness loads increased in phase. The seat-belt and shoulder-harness forces reached their maximum values concurrently with the maximum longitudinal deceleration of the chest. The total seat-belt restraining forces reached a maximum of 2440 pounds at the same instant (0.082 sec) as the shoulder-harness forces reached their maximum value of 1240 pounds. The total restraining forces of the seat belt and shoulder harness would be the sum of these two, or 3680 pounds. The total seat-belt force accounts for approximately

two-thirds of the total restraining force, while the shoulder harness sustained one-third of the total force. The largest stresses, therefore, are on the dummy's pelvic-abdominal region, where they exceed 1 ton. It can be seen from this data that the total restraining force was equally distributed through the three points of attachment of the seat belt and shoulder harness on the airplane structure. The use of the shoulder harness reduced the total restraining force imposed on the seat belt and its attaching structure by approximately 33 percent, and it transmitted this portion of the total restraining force to a different point of the fuselage structure. Part of the decelerative force acting on the dummy is transmitted through its legs, which are in contact with the fuselage frame. Application of this force, which varies in magnitude as the airplane structure deforms, partially accounts for the difference between the shoulder-harness and seat-belt loads after 0.09 second.

It can be seen from figure 11(b) that, as the chest deceleration decreased from its peak value, the total seat-belt force decreased in phase with the decrease in chest deceleration. Meanwhile, the restraining forces on the shoulder harness remained at nearly maximum value. The fact that these restraining forces remained for approximately 0.04 second before decreasing may be due to the rigidity of the leg joints of the dummy, so that the dummy pivoted around the seat belt with his legs pushing against the torso and thus relieved some of the force on the seat belt.

60-Mph crash. - Figure 11(c) is a plot of the harness restraining forces and longitudinal chest deceleration that occurred during the 60-mph crash. These curves show the same characteristics as were noted in the 42-mph crash, except that peak decelerations and peak forces were higher in the 60-mph crash. Total seat-belt force and shoulder-harness force increased in phase with the increase in longitudinal chest deceleration. The total seat-belt force reached a maximum of 4050 pounds approximately 0.003 second after the first peak in chest deceleration of 34g. Maximum shoulder-harness force reached 2050 pounds at 0.085 second after impact. Total restraining force reached a peak value of 5800 pounds. Shoulder-harness force remained at nearly maximum value, while total seat-belt force dropped to 1400 pounds and then built up to a second peak of 3200 pounds. The third peak in longitudinal deceleration reached 50g at 0.120 second after impact.

47-Mph crash. - The dummy was restrained in the 47-mph impact crash by a 2-inch-wide commercial seat belt. No shoulder harness was employed. On the basis of the static elongation and failure tests of the 2-inch-wide seat belt, the belt was expected to fail in this crash. This seat belt was installed on the dummy in order to observe the nature of the

failure in the crash, since friction between the belt and the clothing of the dummy modifies the belt fiber stresses in a way not well understood at the present time. A second seat belt, 3 inches wide, was used in conjunction with the 2-inch-wide seat belt. This 3-inch-wide seat belt was adjusted so that its length was 8 inches longer than the commercial 2-inch-wide seat belt. Figure 14(a) shows an exaggerated view of the length of the seat-belt assembly prior to installation on the dummy in the airplane. With this arrangement, both belts being attached to tensiometers, a continuous recording of the belt forces was obtained up to and following the breaking of the 2-inch-wide seat belt.

Figures 14(c) and (d) illustrate the relation of total seat-belt force to vertical and longitudinal accelerations in the 47-mph crash. The vertical and longitudinal chest-acceleration curves are shown in figure 14(c); the curve of longitudinal chest deceleration is plotted with the total seat-belt force in figure 14(d).

Total seat-belt restraining force (fig. 14(d)) reached a maximum of 4400 pounds as the longitudinal chest deceleration reached a peak of 45.5g. Total seat-belt force increased in phase with longitudinal chest deceleration and decreased in phase with the decay in longitudinal chest deceleration from its final peak.

Three peak values appeared in the curve of longitudinal chest deceleration, while the seat belt had only two peak values. The three peaks in longitudinal chest deceleration occurred because the torso was allowed a wide range of movement during deceleration. Because the restraining force was applied with only a seat belt, the belt acted as a fulcrum about which the torso was allowed to rotate. Between the onset of deceleration and the decay from the final peak in deceleration, response of the torso to the restraining force is indeterminate.

The sharp drop in the total seat-belt force is due to the failure of the 2-inch-wide seat belt between 0.084 and 0.094 second after impact and the subsequent loading of the 3-inch-wide seat belt. Failure of the 2-inch seat belt is indicated by the rapid rate of decay from the peak load (0.084 sec after impact). The time during which this sharp drop in total seat-belt force occurred (0.006 sec) indicates progressive failure of the fibers of the belt webbing from the cutting action of the buckle. Figure 14(b) is a post-crash photograph showing the break in the 2-inch seat belt and the undamaged 3-inch seat belt.

In sustaining a peak force of 4400 pounds, before failure in the 47-mph crash, the 2-inch seat belt had withstood 147 percent of the breaking force recorded for an identical belt during the static tensile-test mock-up (fig. 13(b)). The seat-belt breaking strength under dynamic loading in the crash was approximately $1\frac{1}{2}$ times as great as the breaking load of 3020 pounds under static loading.

Vertical chest accelerations in figure 14(c) support the indication that the 2-inch seat belt broke between 0.084 and 0.092 second. The change of direction recorded in the vertical chest acceleration during this time indicates that as the first seat belt broke, it allowed the dummy to travel upward, unrestrained, until the dummy contacted the second seat belt. As soon as the dummy contacted the second seat belt, his momentary upward travel was arrested, as shown by a decrease in upward acceleration. Beginning at 0.093 second, the total seat-belt force increased in phase with the change in vertical acceleration.

The motion-picture data showed that the dummy started moving forward from his seat at 0.041 second. This time concurs with the dummy movement indicated by the longitudinal chest deceleration. At 0.091 second, the dummy started to flex around the 3-inch seat belt after the 2-inch seat belt had broken.

The drop in total seat-belt force to a value of 1500 pounds at 0.091 second indicates that the 8-inch slack in the 3-inch-wide seat belt was not completely taken up at the time of failure in the 2-inch seat belt. After the 2-inch seat belt had failed, the remaining force of deceleration was absorbed by the 3-inch seat belt. Maximum displacement of the pelvic region of the dummy was reached at 0.112 second after impact, because the displacement consisted of the accumulated elongation of both seat belts.

Maximum bending of the torso about the seat belt did not appear until 0.139 second, or 0.027 second after maximum displacement of the pelvic region of the dummy. Removal of the front seat for this test permitted full flexion of the torso around the seat belt. Maximum bending of the torso was delayed until the longitudinal chest deceleration had decreased to values of 7 to 8g.

Survivability Aspects - Injury Potential

Deceleration. - The conclusions reached from the work on "Human Exposures to Linear Deceleration" (ref. 3) were that the severity of the physiological damage during deceleration depends on the magnitude, the rate of increase, and the duration of the deceleration.

In the study described in reference 3, a human being, carefully supported in his seat by a specially designed seat-belt - shoulder-harness - leg-strap combination, was subjected to a maximum deceleration of 45.3g, existing for a duration of 0.228 second, with a rate of onset of deceleration of 493g per second. The injury sustained in this deceleration consisted of conjunctival and retinal hemorrhage. These injuries were not of sufficient intensity to prevent continuance of normal duties following the test. Definite signs of shock were noted in

the same investigation at a plateau value of 38g, when the rate of onset of deceleration was increased to 1370g per second. These values of maximum deceleration, time of duration, and rate of onset of deceleration were the data obtained from the time-displacement data on the sled (ref. 5) on which the human being rode; consequently, they represent only the maximum values employed in the study and do not define the absolute limits of human tolerance. The chest deceleration measured in the crashes reported herein were no higher than the value of 45.4g obtained in the study in reference 3. A peak value of 50g of short duration, however, was obtained during the 60-mph crash. In investigations of actual stall-spin accidents conducted by Cornell Crash Injury Research, in which the distortion of the airplane structure was equal to, or exceeded, that obtained in the 60-mph crash, the rear passenger was frequently found to survive. The 50g peak in deceleration is therefore assumed to be survivable.

Rate of onset of deceleration varied in the light-airplane crashes from 1000 to 2500g per second. The 1370g per second rate of onset of deceleration used in the studies with human beings is exceeded in some of the crashes of this study. It is difficult, however, to appraise the full meaning of this fact in terms of human survival, since the duration of onset of deceleration was much briefer in the crashes reported herein than in the tests in reference 3.

Bodily contact with structure (seat belt - shoulder harness). - Comparison of the relative forward movement of both dummies during the 42-mph crash illustrates the limited forward movement of the occupant when shoulder harness is worn in addition to the normal seat belt. As seen in figure 15, the rear dummy (installed with seat belt and shoulder harness) moved forward out of his seat about 8 to 10 inches, the forward displacement being limited to the amount of elongation in the webbing of the restraining harnesses. In the most forward position, reached at 0.089 second, the torso was approximately vertical. During this time, the front dummy (installed with seat belt only) also moved forward out of its seat about the same distance, with the torso reaching the vertical position. The torso of the front dummy then pivoted around the seat belt about 30° past the vertical position, until the forward movement, or rotation, or both, was arrested by the dummy's striking the instrument panel. At 0.116 second (fig. 15(b)), the dummy's chest contacted the face of the instrument panel, and its chin contacted the top of the instrument panel. The maximum forward position of the dummy shows that the chest of the front-seat occupant in this airplane had been thrown 22 to 24 inches forward from its normal seated position to strike the instrument panel because it was not held tightly with seat-belt - shoulder-harness restraint.

The front dummy in the 60-mph crash also struck the instrument panel in the same manner as illustrated for the 42-mph crash. The front dummy in both crashes then bounced back into the normal seated position as shown by the post-crash photographs of the 60- and 42-mph crashes in figure 16. These figures, when compared with the photograph of an undamaged airplane (fig. 3), also illustrate the reduction in distance between the front dummy and the instrument panel. The post-crash front-cockpit clearance decreased as impact speed increased.

Figure 17(a) is a front view of the dummy, indicating the location and the areas of contact in the 60-mph crash. Contact of the head with the instrument panel was of sufficient intensity to put permanent creases in the heavy canvas covering of the dummy's head. The head struck the top of the instrument panel over the two areas indicated in figure 17(a) and left the dent in the instrument panel as shown in figure 16(a). The right-side view of the head in figure 17(b) shows the area over which the head contacted the upper right cabin diagonal brace on the rebound. Contact of the chest with the face of the instrument panel over the area indicated (fig. 17(a)) was of sufficient force to imbed numerous pieces of metal in the felt-fabric covering of the dummy. Definite contact with the control stick was indicated in the position shown in figure 17(a). Final position of the control stick with respect to both the dummy's chest and the instrument panel is shown in figure 16(a). This figure also shows the final position of the knees jammed into the bottom edge of the instrument panel. Figure 17(a) indicates areas on the knees of the dummy that were cut and torn by this contact. Abrasion marks on the cloth covering of the dummy's lower legs indicate contact with the lower-cabin removable diagonal braces. The final position of both feet in figure 17(b) indicates the severe flexure of both ankles in the crumpled forestructure, while the back view shows the area on the back of the neck struck by the helmet of the rear dummy.

A recent statistical analysis (ref. 6) shows that of 800 accidents that were considered survivable, injuries of the head were more frequent than injuries of any of the five remaining gross body areas. Head injuries were sustained in 88 percent, or 704, of the 800 accidents analyzed. With regard to the occurrence of fatal injuries in accidents involving aircraft of all types, German accident statistics (ref. 7) reveal that 50 percent of all injuries were injuries of the head, and that 70 to 80 percent of the fatal injuries were caused by injuries of the head. When the areas over which the front dummy contacted structure in the 60-mph crash (fig. 17) are considered, the statistics on human injury incurred by this sort of contact in actual accidents are quite understandable.

Bodily contact with structure (seat belt only). - In order to investigate the sequence of events during displacement of the torso around the seat belt, the anthropomorphic dummy was installed in the rear seat with only seat-belt restraint in the 47-mph crash. To provide unlimited movement of the torso about the seat belt, the front seat and the rear control stick were removed. Photographs in figure 18 of the 47-mph crash show the movement of the dummy forward out of its seat, followed by rotation of the torso about the seat belt. Without the control stick and the front seat to limit the movement of the torso and the head, the torso rotated forward and downward until the chest contacted the thighs at 0.118 second after impact (fig. 18(b)). The distance through which the torso and the head swung around the seat belt into the area forward of the dummy was approximately the length of the torso from the hips to the top of the head. It is apparent from figure 18 that, if injuries resulting from contact with solid structure are to be avoided when using only seat-belt restraint, the estimated distance of 31 to 45 inches (ref. 7) forward of the seat must remain free of any solid, sharp, or unyielding protuberances.

Collapse of cabin structure. - Potential injury of the occupants due to inward-collapsing cabin structure is indicated by comparison of the extent of the collapse of the cabin structure in figure 19. The figures show photographs of the cabin area following the 42-, 47-, and 60-mph crashes. As indicated by comparison of these photographs, an increase of speed at impact with the barrier caused a corresponding reduction of the volume enclosed by the cabin structure. Figure 19(a) shows that, during the 42-mph crash, deformation of the cabin was minor. Appreciable reduction in cabin volume was noticeable with an increase of impact speed to 47 mph. During this crash, the cabin volume was reduced by the rearward displacement of the instrument panel, as may be detected by comparing the position of the upper, forward, right-side diagonal brace in figure 19(b) with its undistorted position after the 42-mph crash, figure 19(a). With an impact speed of 60 mph, considerable reduction in cabin volume resulted. This reduction resulted from (1) rearward movement of the instrument panel nearly to the front dummy's chest and (2) collapse of the longerons under the rear seat (fig. 19(c)). Distortion of the cabin structural tubing during cabin deformation may increase the probability of injury to the occupants. An example of this distortion is shown by the upper cabin members projecting into the proximity of the heads of both dummies in figure 19(c). It is evident from inspection of figure 19 that, if occupants of an airplane during a crash are to be protected from the additional hazard of striking the deformed cabin structural members collapsing around them, the cabin structure itself must be strong enough to resist the decelerative forces occurring at impact.

Fire hazard. - To permit some insight into the possibility of the occurrence of fire after crash, the distribution of fuel spillage during a crash was investigated during the 60-mph crash. In this crash, the fuel tank contained 8.7 gallons (75 percent of its volume) of red-dyed water to replace the weight of the normal 12-gallon supply of gasoline.

Figure 20 shows the damage to the fuel tank in the 60- and 42-mph crashes. In each crash the fuel tank was crushed between the fire wall and the instrument panel. In the 60-mph crash, the tank was burst at the seams and the sheet metal was torn open by hydraulic loading. The tank was compressed to one-half of its original volume in the crash. Figure 20(b) shows that the empty tank was only deformed and crushed, with no bursting of the seams and no tearing of the parent sheet metal, in the 42-mph crash.

The fuel-spread pattern (fig. 21) of the 60-mph crash reveals a heavy concentration of fuel around the engine, throughout the cabin, and over approximately 66 percent of the under surface of the right wing. The fuel spillage within the passenger compartment and on both dummies, if ignited, would have completely inflamed their clothing. In the two crashes in which a dummy was installed in the front seat, the manner in which its foot was pinned in the wreckage indicates that, if fire were to occur, a human occupant in the same position would experience extreme difficulty in extricating himself before fire enveloped the entire airplane. Figure 16 shows the front dummy's foot pinned between the fire wall and the right-side removable diagonal brace.

If this fuel spillage is typical of that occurring during an actual accident with airplanes having fuel tanks in a location similar to those used in these crashes, a disastrous fire would result if ignition occurred. CAB statistical analysis of the first 3000 non-air carrier accidents reported in 1952 (ref. 8) shows that, of 2344 accidents involving airplanes used for instructional purposes, pleasure flying, and personal transportation, approximately 3.84 percent caught fire after crash. Fortunately, ignition sources of sufficient intensity to ignite gasoline do not appear consistently with this type of engine installation.

SUMMARY OF RESULTS AND CONCLUSIONS

The results obtained from the full-scale light-airplane crash investigation, in which stall-spin accidents were simulated, are summarized in the following table:

Speed at impact with barrier, mph	Maximum longitudinal engine deceleration, g	Maximum longitudinal deceleration of chest of rear dummy, g	Maximum longitudinal deceleration of fuselage under rear seat, g	Duration of maximum peak longitudinal deceleration of fuselage at rear seat, sec	Peak total restraining force, rear dummy, lb
42	32.5	32	26.5	0.023	3680
47	46.0	46	32.5	.038	4400
60	62.0	50	33.5	.070	5800

These data show that, for the stall-spin accident simulated:

1. Longitudinal deceleration of the chest of the dummy in the rear seat ranged from 32 to 50g when the crash impact speed varied from 42 to 60 mph.

2. Peak longitudinal chest deceleration exceeded longitudinal fuselage-floor deceleration by 6 to 16g in all crashes.

3. Deceleration of the fuselage at the rear-seat location did not increase appreciably (26 to 33g) as impact speed increased from 42 to 60 mph, but the time during which significant deceleration persisted increased from 0.023 to 0.070 second.

4. Total peak force imposed on the restraining harnesses increased in proportion with the increase of impact speed and reached a maximum of 5800 pounds in the 60-mph crash.

5. Occupants of airplanes of the type used in this investigation would not be endangered by deforming cabin structure unless crash impact speeds exceeded 42 mph.

6. The results of this study show that the decelerations imposed by this airplane and crash configuration up to impact speeds of 60 mph, with the rear-seat occupant restrained by seat belt and shoulder harness, are within the decelerations shown by aeromedical research to be tolerable by human beings.

7. In order to avoid injury-producing contact when only seat-belt restraint is used, the space in front of the occupant must remain free of obstacles for a distance approximately equal to the length of the torso from the hips to the top of the head (plus the seat-belt elongation).

8. The maximum total restraining forces recorded indicate that, when seat-belt restraint is used alone, these belts should be capable of withstanding higher breaking loads than those presently in use. All components of the restraining harness system should be attached to the basic airframe structure, unless the seat and its attachment are capable of withstanding the restraining forces.

Lewis Flight Propulsion Laboratory
National Advisory Committee for Aeronautics
Cleveland, Ohio, May 11, 1953

REFERENCES

1. DeHaven, Hugh: The Relationship of Injuries to Structure in Survivable Aircraft Accidents. Rep. No. 440, National Res. Council, Div. Medical Sciences for Committee on Medical Res. of Office Aviation Medicine, July 9, 1949.

2. Black, Dugald O.: Facilities and Methods Used in Full-Scale Airplane Crash-Fire Investigation. NACA RM E51L06, 1952.

3. Stapp, John Paul: Human Exposures to Linear Deceleration. Part 2. The Forward-Facing Position and the Development of a Crash Harness. AF Tech. Rep. No. 5915, Part 2, U. S. Air Force, Wright Air Dev. Center, Wright-Patterson Air Force Base, Dayton (Ohio), Dec. 1951.

4. Wurzel, Edward M., Polansky, Lewis J., and Metcalfe, Earl E.: Measurements of the Loads Required to Break Commercial Aviation Safety Belts as an Indication of the Ability of the Human Body to Withstand High Impact Forces. Rep. No. 12, Naval Medical Res. Inst., Bethesda (Maryland), Mar. 16, 1948. (Proj. MN 001 006 X-630.)

5. Denzin, E. C.: A Decelerator for Human Experimentation. AF Tech. Rep. No. 5973, U. S. Air Force, Air Materiel Command, Wright-Patterson Air Force Base, Dayton (Ohio), Feb. 1950. (Air Force Contract (33-038)ac-15227.)

6. Crash Injury Research: The Site, Frequency and Dangerousness of Injury Sustained by 800 Survivors of Lightplane Accidents. Dept. Public Health and Preventive Medicine, Cornell Univ. Medical College, New York (N.Y.), July 1952. (Office Naval Res. Contract N6onr 264-12.)

7. U. S. Air Force: German Aviation Medicine - World War II. Vol. 1. Dept. Air Force, 1950.

8. Civil Aeronautics Board: Non-Air Carrier Accident Trends. Jan. 15, 1953.

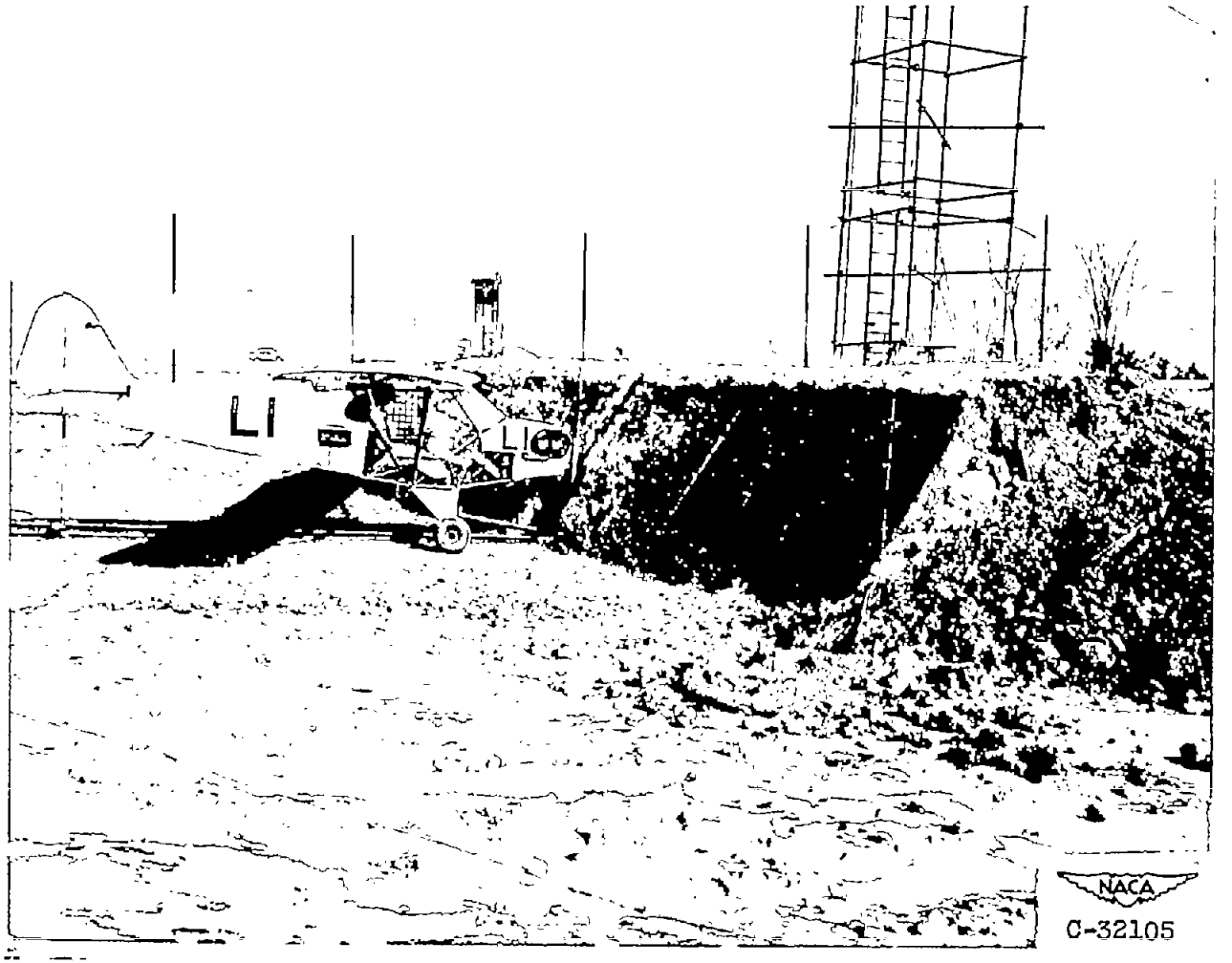

(a) Photograph of two-seat tandem airplane used in investigation, showing relation of airplane engine and left wing to front edge of earthen crash barrier.

Figure 1. - Mechanism for light-airplane crash investigation.

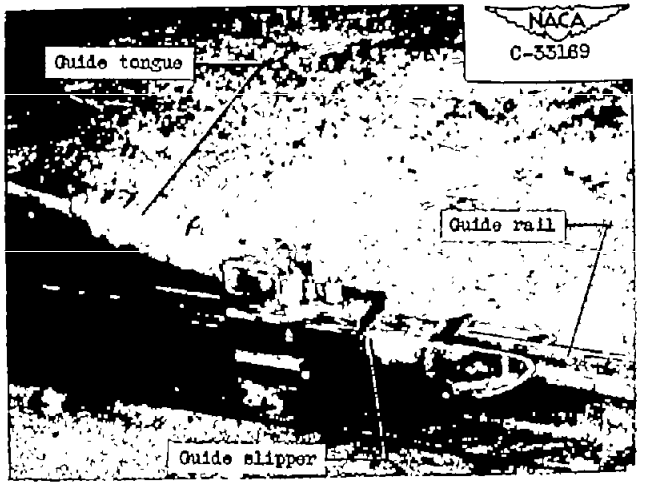

(b) Guide slipper and guide tongue assembly installed on guide rail.

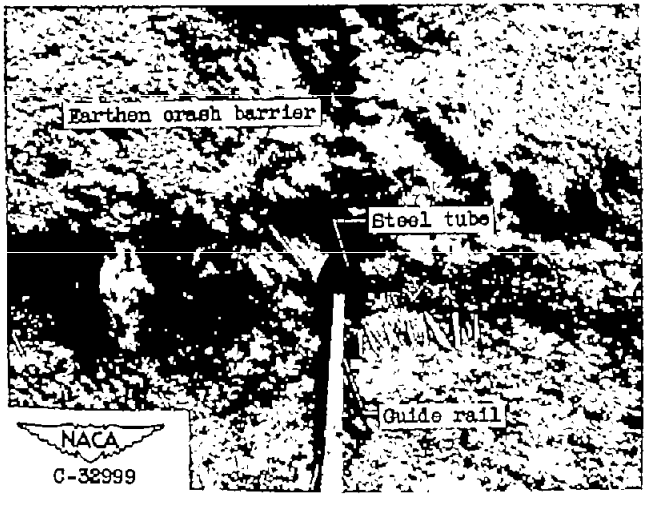

(c) Steel tube installed at base of crash barrier for disposal of guide tongue and slipper assembly.

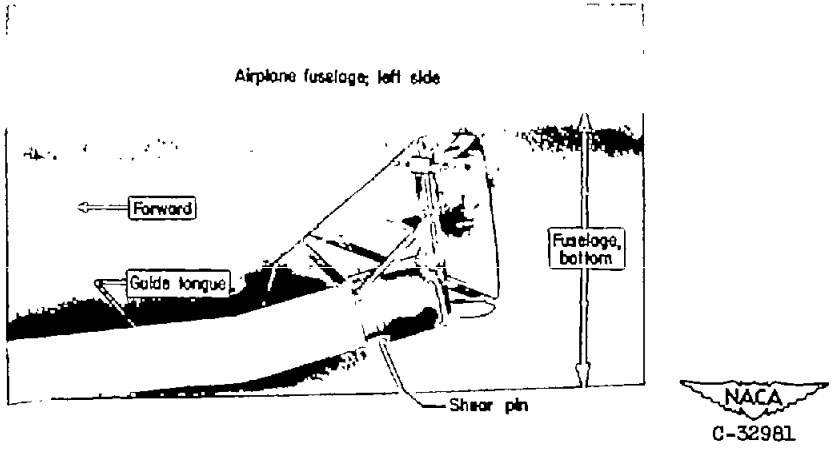

(d) Attachment of tongue to fuselage, showing shear-pin location.

Figure 1. - Continued. Mechanism for light-airplane crash investigation.

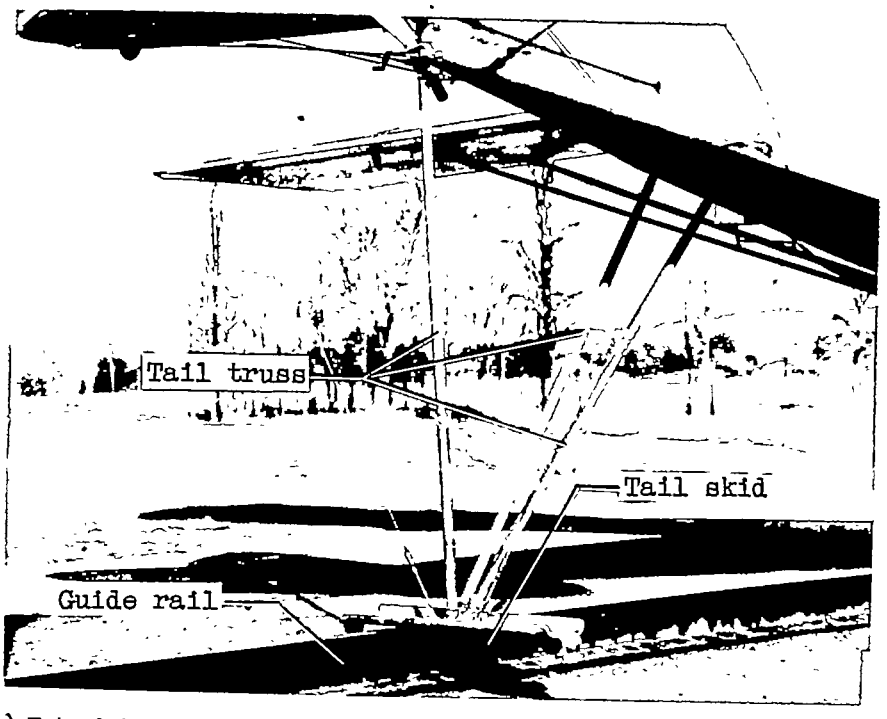

(e) Extended tail-truss support for holding airplane in flight attitude.

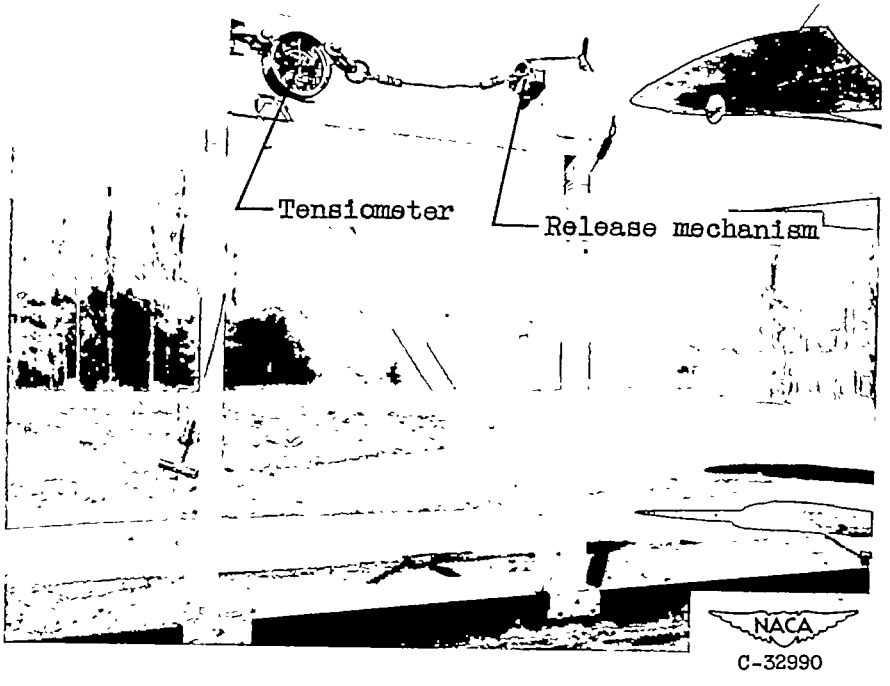

(f) Anchor pier installed on guide rail to retain airplane before release.

Figure 1. - Concluded. Mechanism for light-airplane crash investigation.

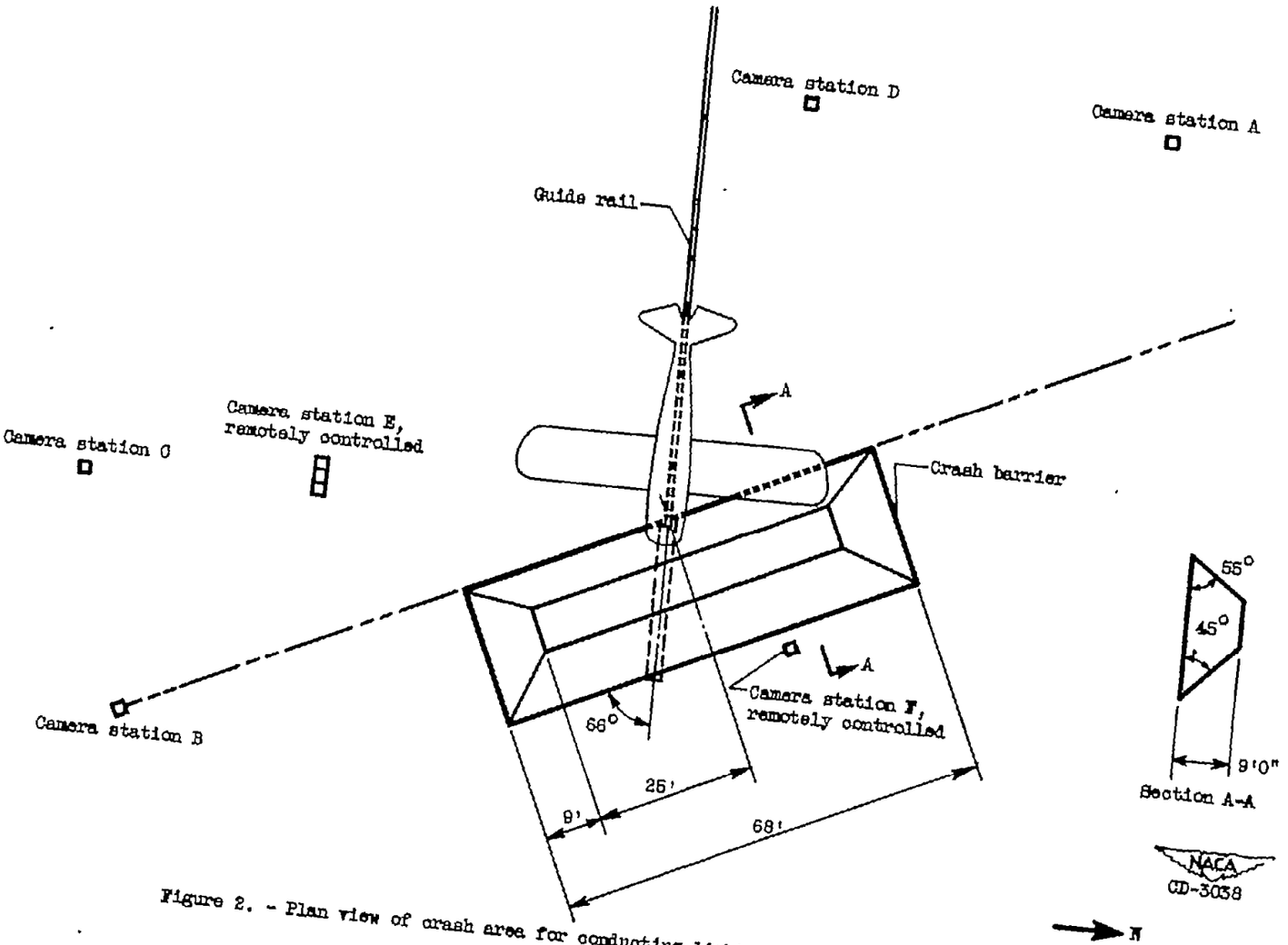

Figure 2. - Plan view of crash area for conducting light-airplane crash investigation.

Figure 3. - Typical installation of anthropomorphic and parachute dummies in airplane.

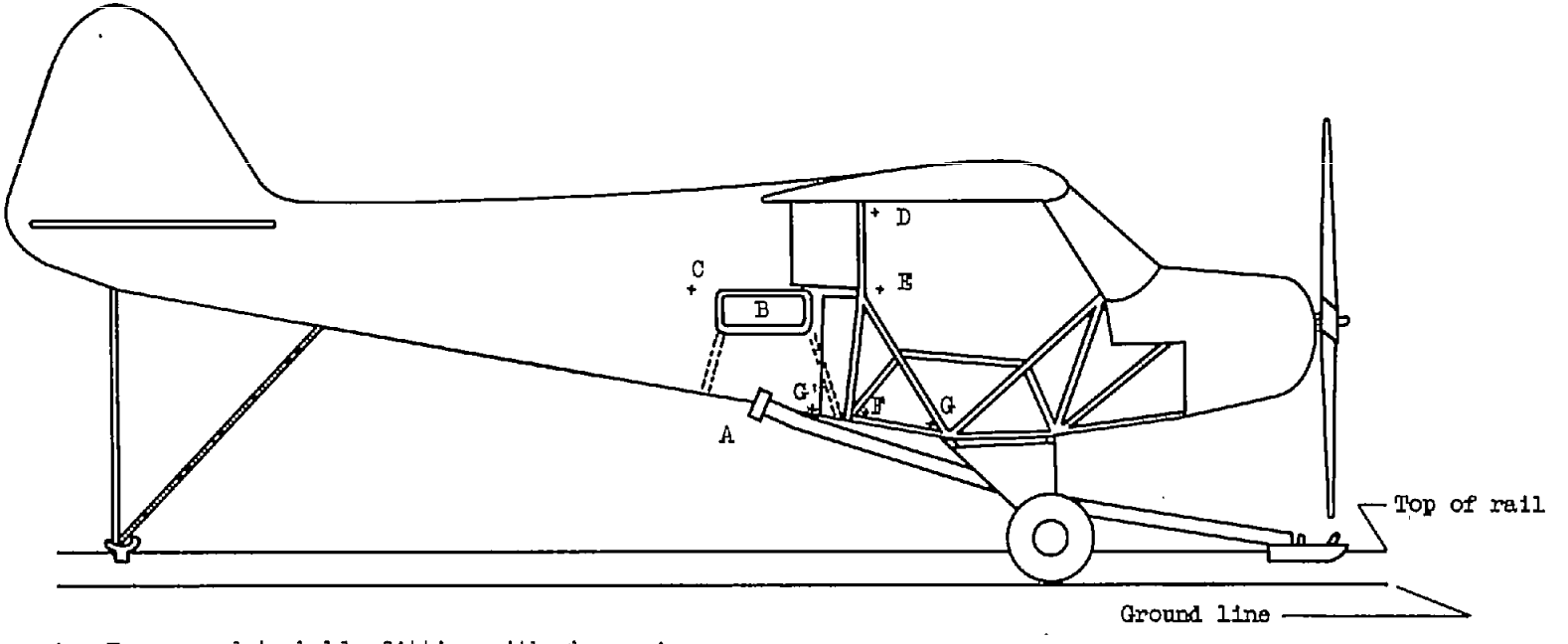

A Tongue - detachable fitting with shear pin
B Mobile telemeter station
C Tensiometer - shoulder harness
D Accelerometer - head
E Accelerometers - chest
F Tensiometers - seat belt
G Accelerometers - floor, 60 mph
G' Accelerometers - floor, 42, 47 mph

NACA
CD-3037

(a) General location of instrumentation in airplane.

Figure 4. - Instrumentation used in light-airplane crash investigation.

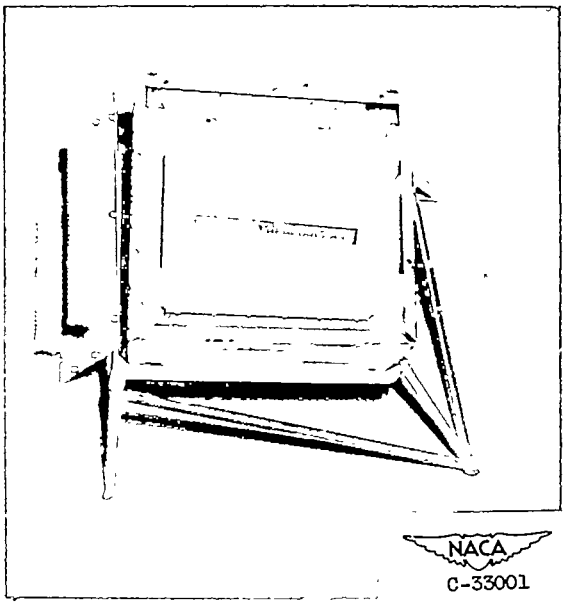

Crash-protection arrangement, top view

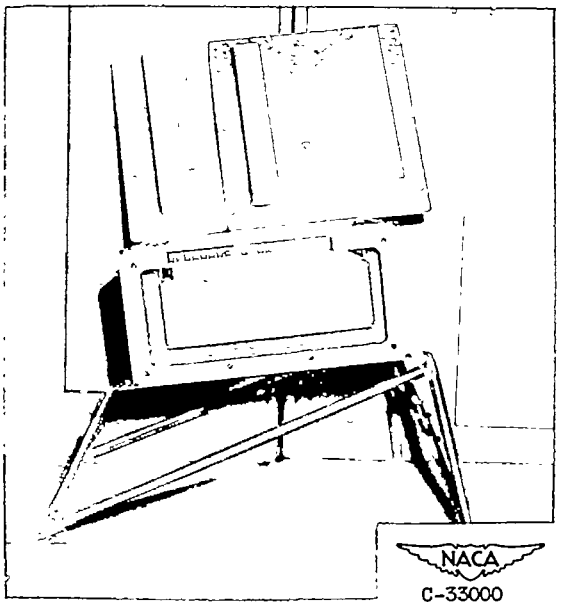

Before installation

Mounted in protective box and installed

(b) Mobile telemeter transmitter station.

Figure 4. - Continued. Instrumentation used in light-airplane crash investigation.

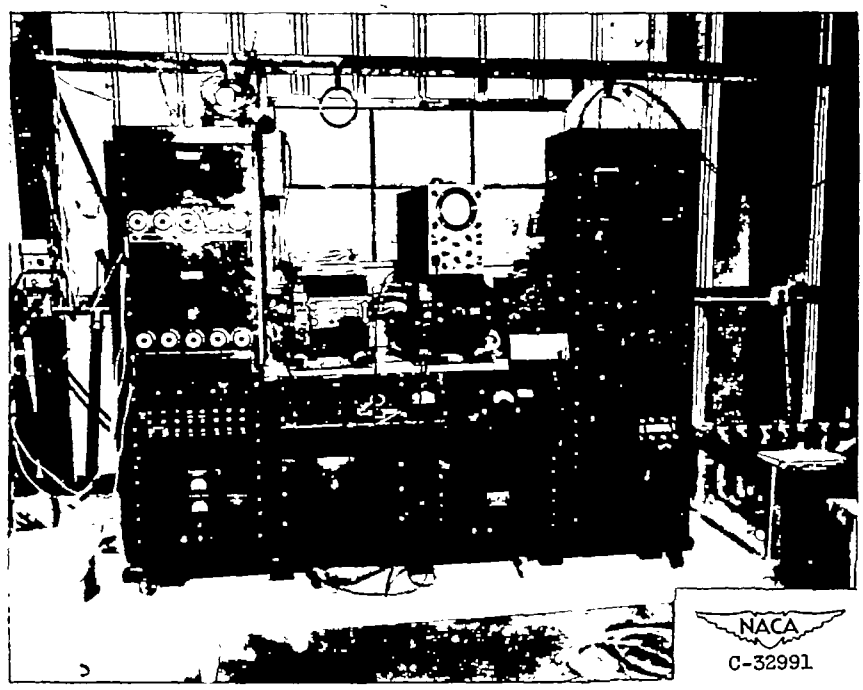

(c) Ten-channel telemeter receiving and recording station.

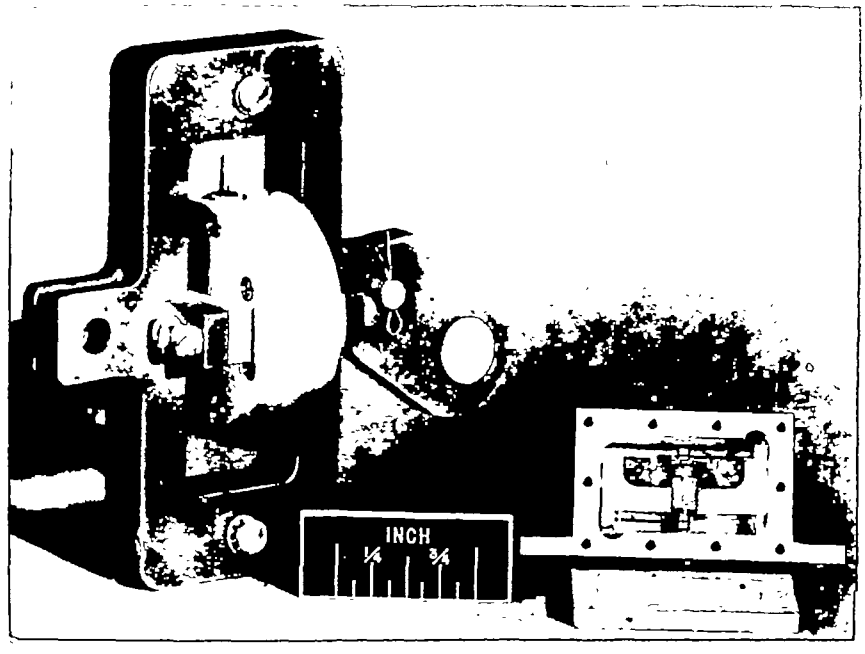

Tensiometer Accelerometer

NACA
C-33003

(d) Telemeter transducers.

Figure 4. - Continued. Instrumentation used in light-airplane crash investigation.

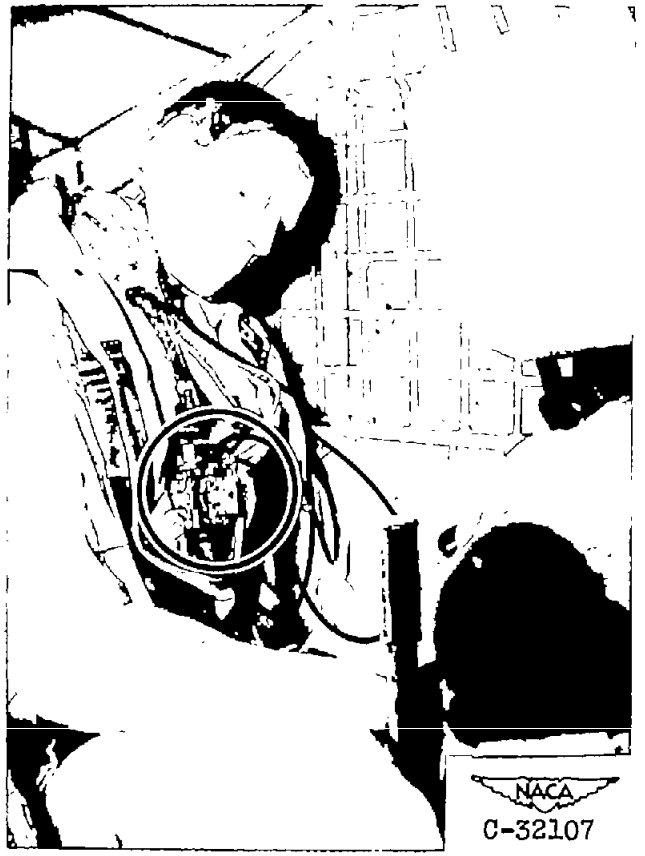

(e) Accelerometers installed on chest of rear dummy.

(f) Accelerometer installed in head of rear dummy.

Figure 4. - Continued. Instrumentation used in light-airplane crash investigation.

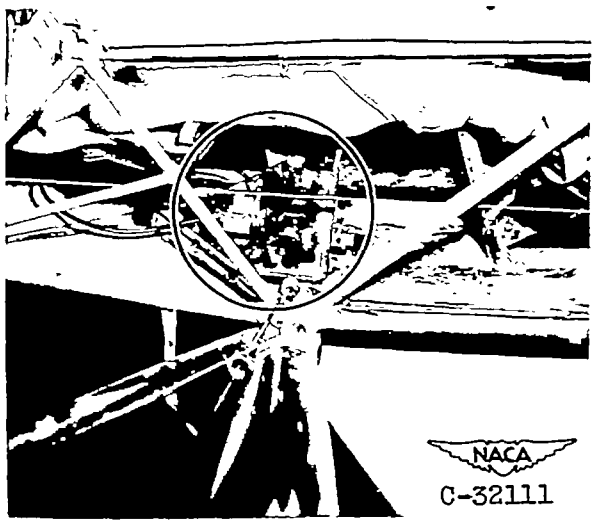

(g) Accelerometers installed on fuselage floor at rear seat in 60-mph crash.

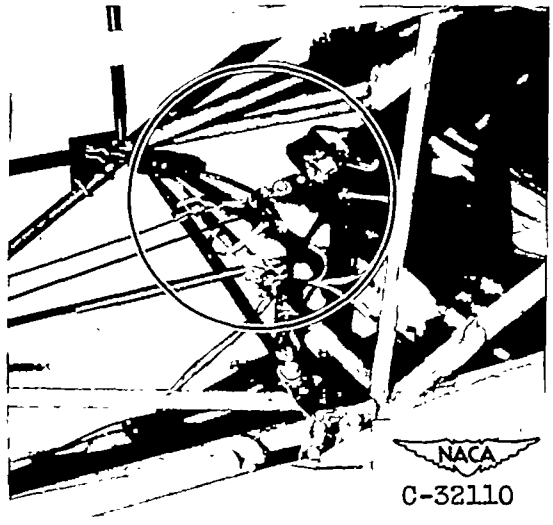

(h) Shoulder-harness tensiometer.

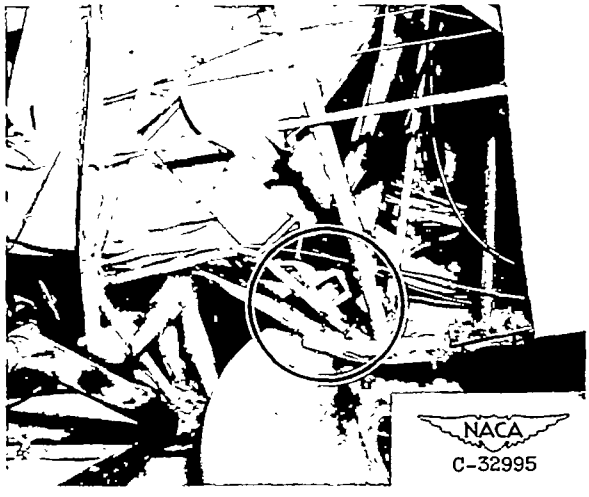

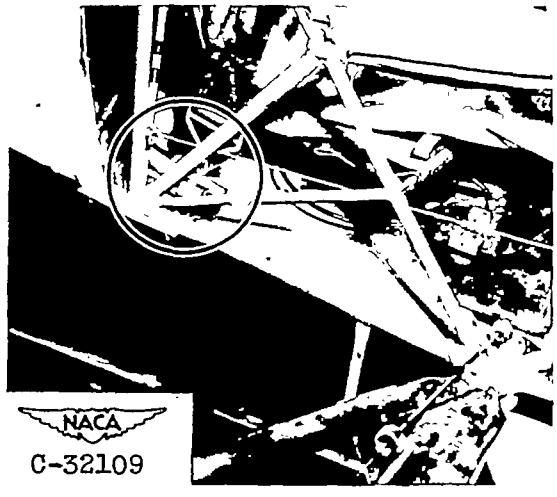

Left (i) Seat-belt tensiometers at rear seat. Right

Figure 4. - Continued. Instrumentation used in light-airplane crash investigation.

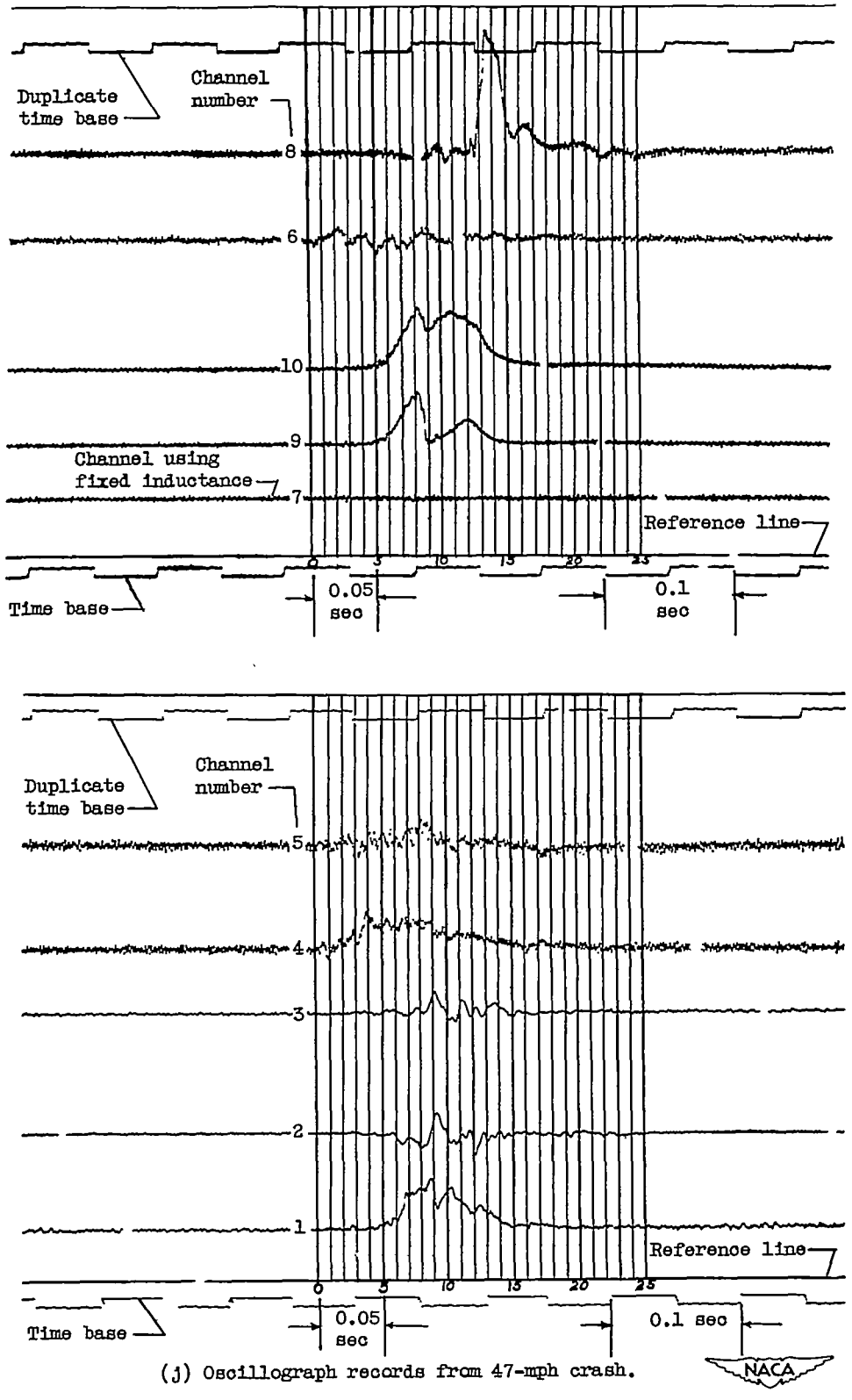

(j) Oscillograph records from 47-mph crash.

Figure 4. - Continued. Instrumentation used in light-airplane crash investigation.

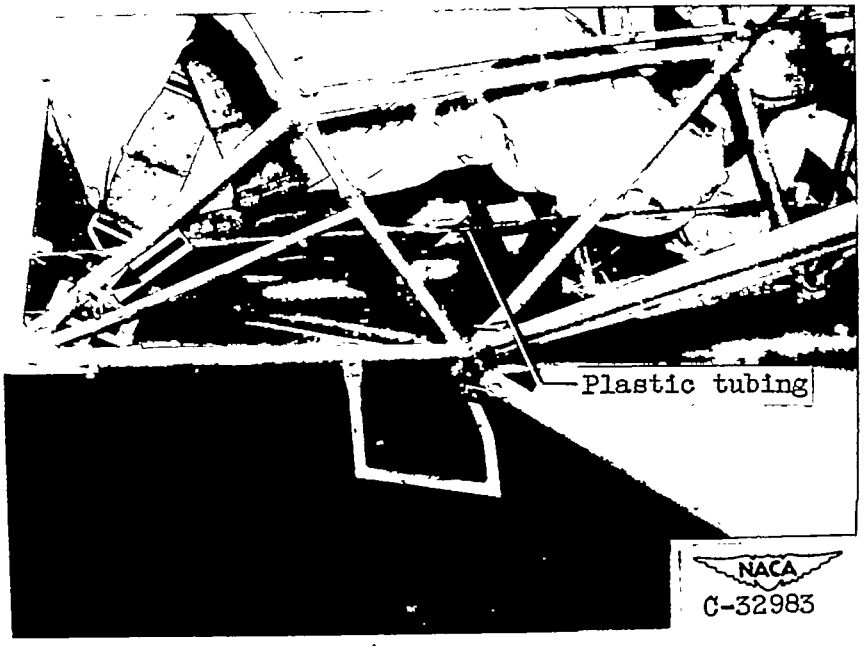

(k) Ground braid, and plastic tubing over control cable, to eliminate extraneous noise.

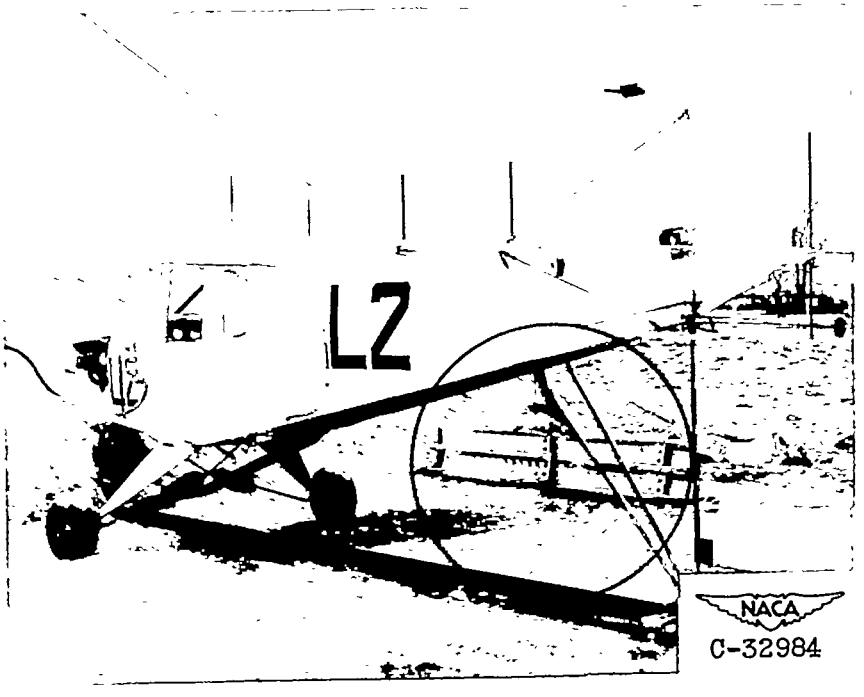

(l) Bank of flash bulbs to provide auxiliary illumination in cabin area during impact.

Figure 4. - Concluded. Instrumentation used in light-airplane crash investigation.

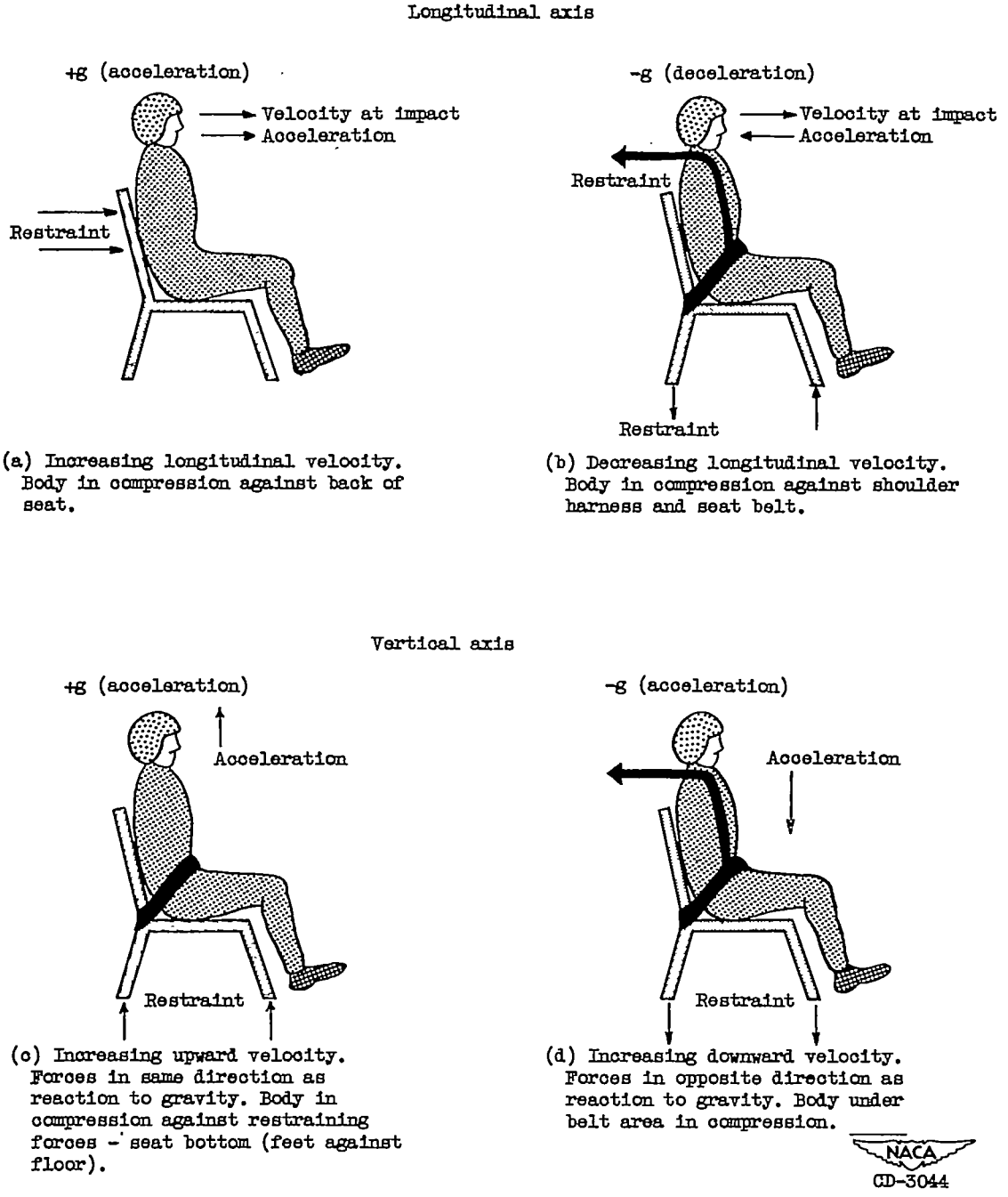

(a) Increasing longitudinal velocity. Body in compression against back of seat.

(b) Decreasing longitudinal velocity. Body in compression against shoulder harness and seat belt.

(c) Increasing upward velocity. Forces in same direction as reaction to gravity. Body in compression against restraining forces - seat bottom (feet against floor).

(d) Increasing downward velocity. Forces in opposite direction as reaction to gravity. Body under belt area in compression.

Figure 5. - Reaction of seated body to longitudinal and vertical accelerations.

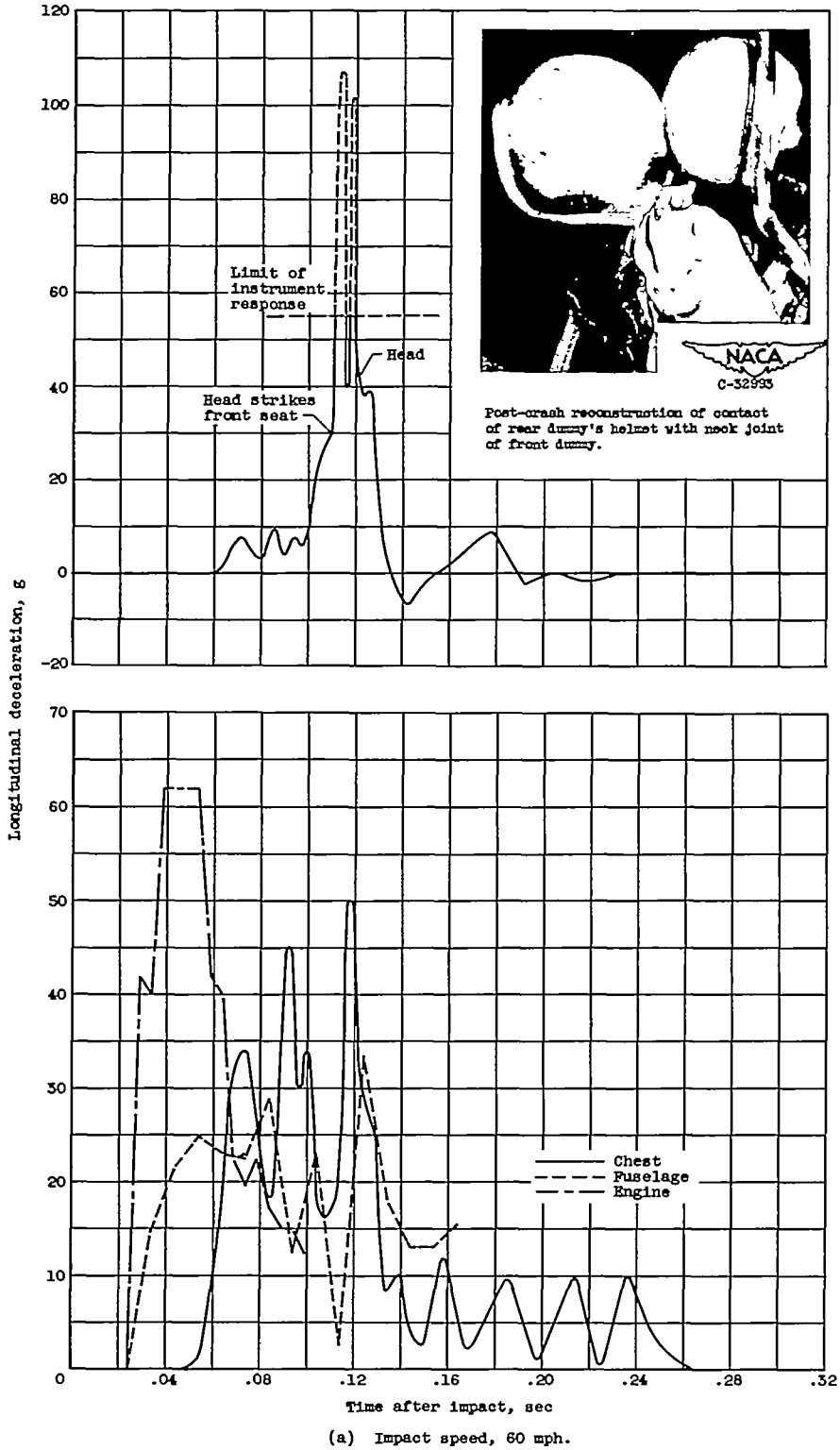

(a) Impact speed, 60 mph.

Figure 6. - Longitudinal deceleration of engine, fuselage floor at rear seat, and chest and head of rear dummy.

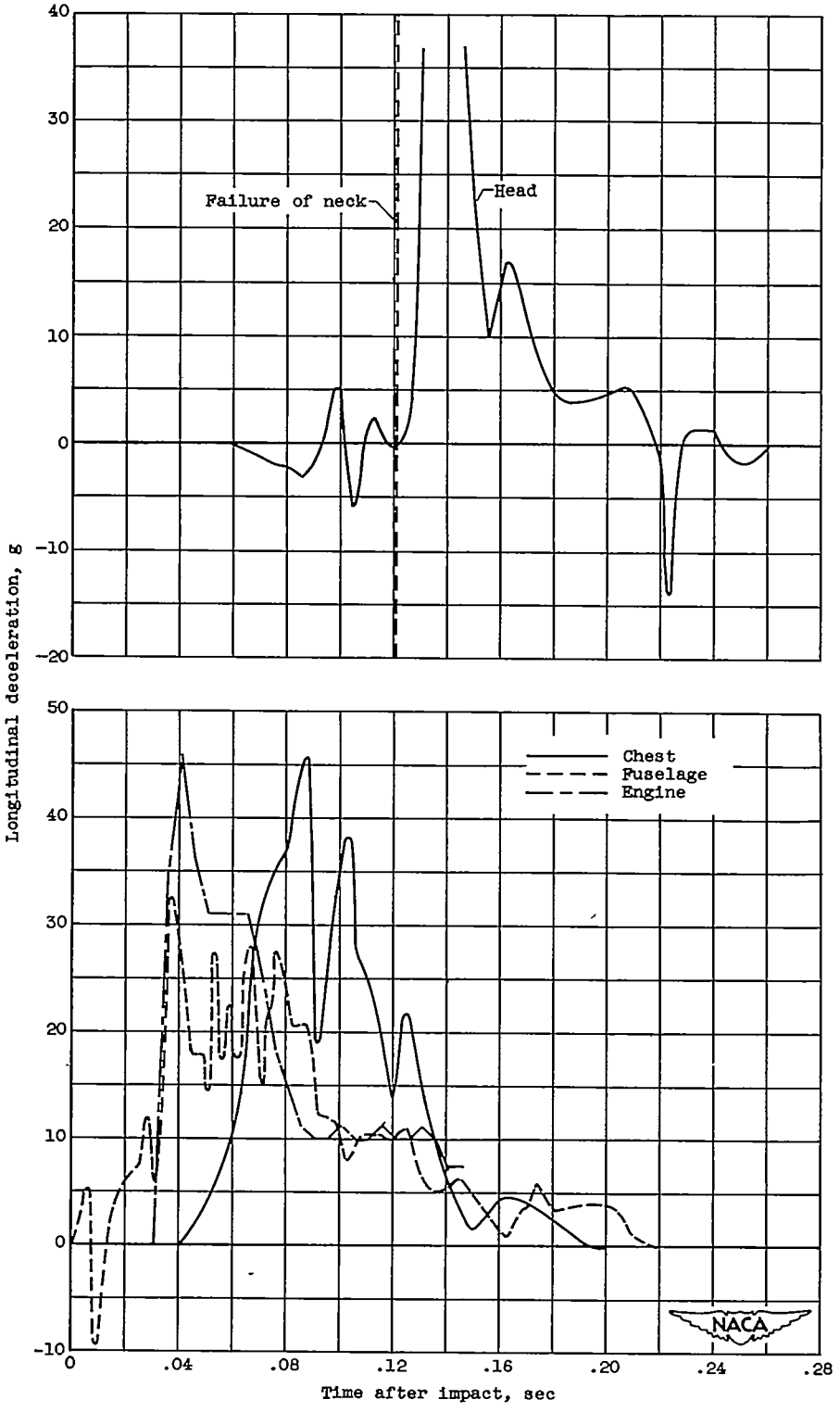

(b) Impact speed, 47 mph.

Figure 6. - Continued. Longitudinal deceleration of engine, fuselage floor at rear seat, and chest and head of rear dummy.

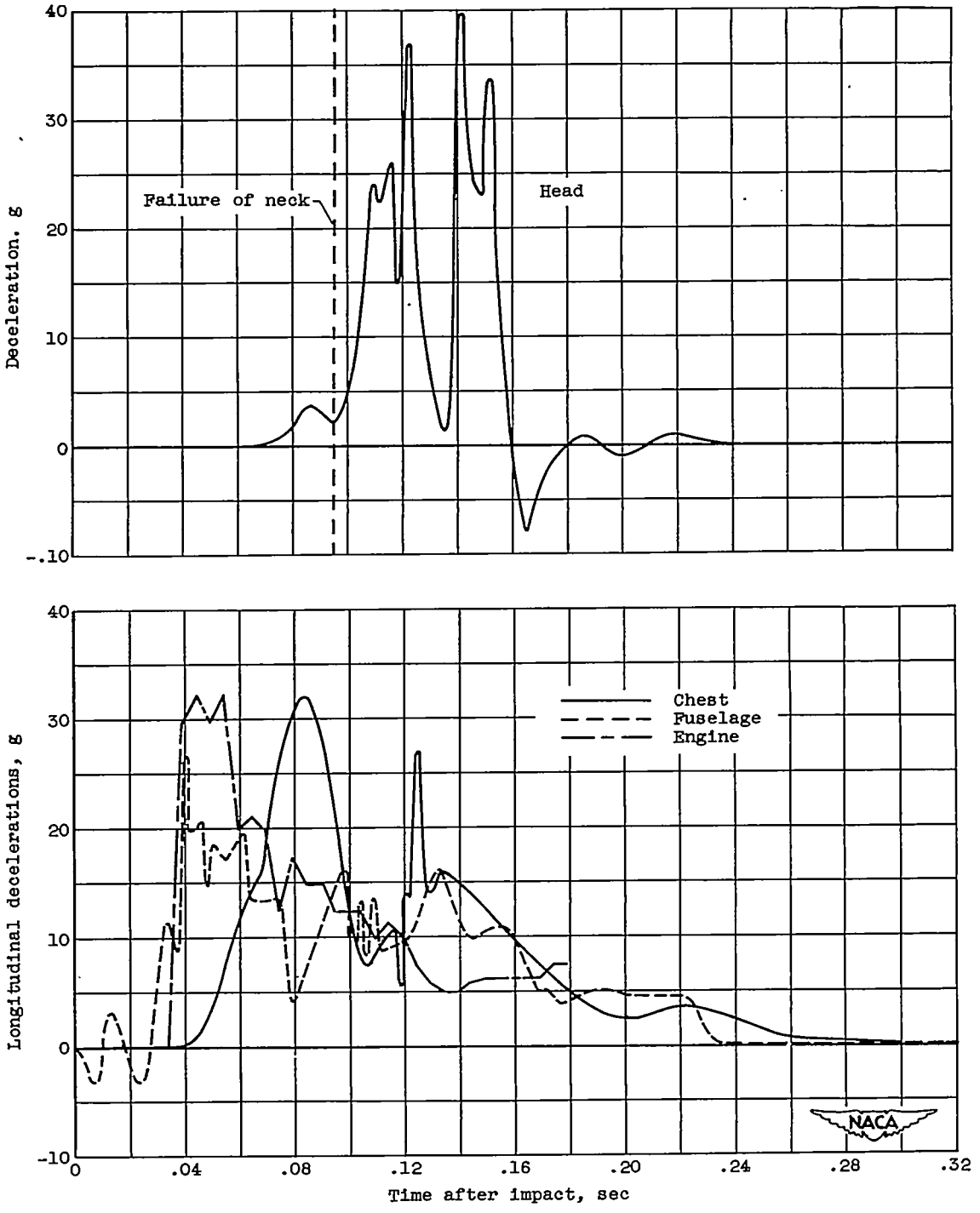

(c) Impact speed, 42 mph.

Figure 6. - Concluded. Longitudinal deceleration of engine, fuselage floor at rear seat, and chest and head of rear dummy.

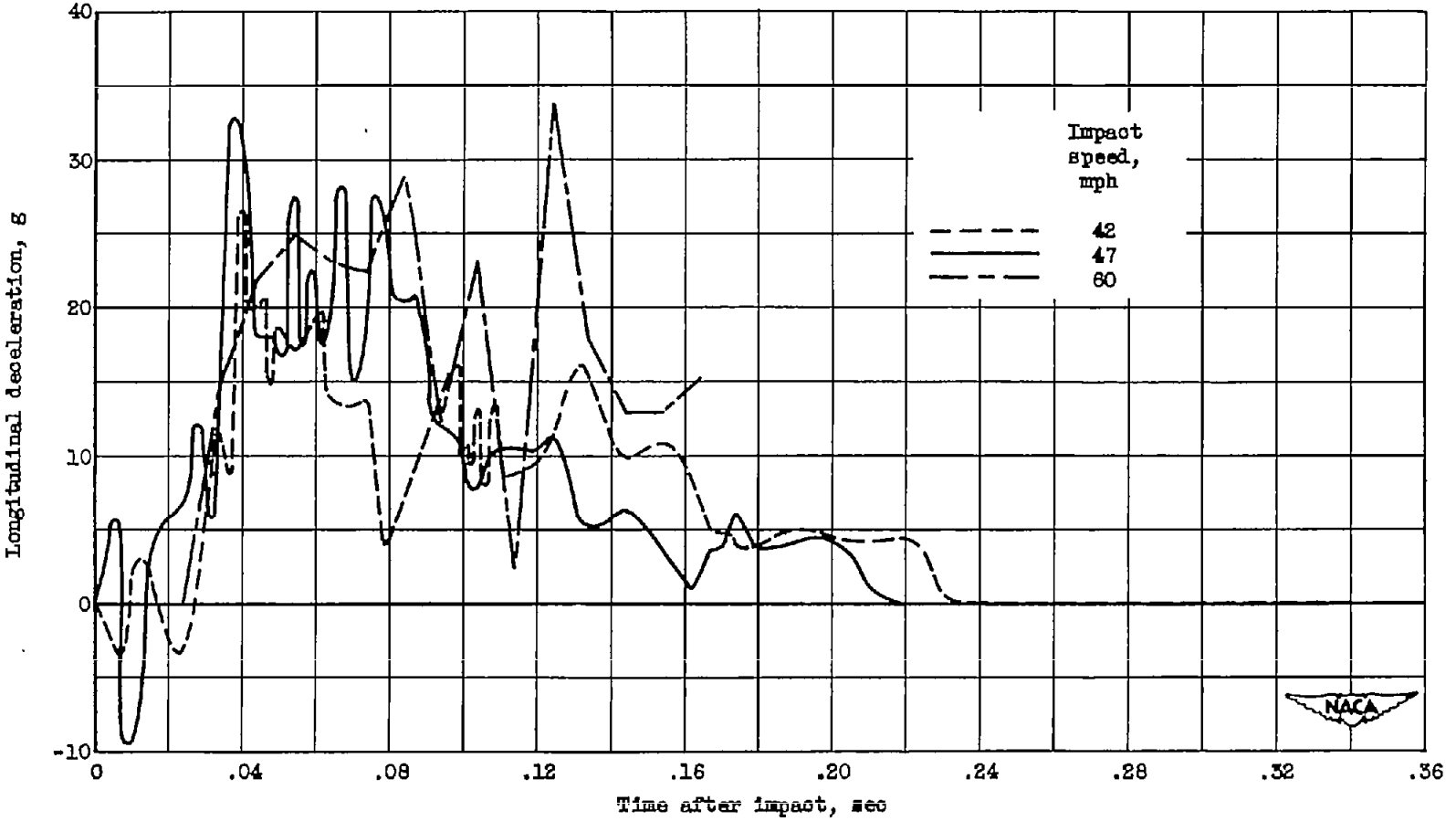

Figure 7. - Effect of impact speed on longitudinal deceleration of fuselage at rear seat.

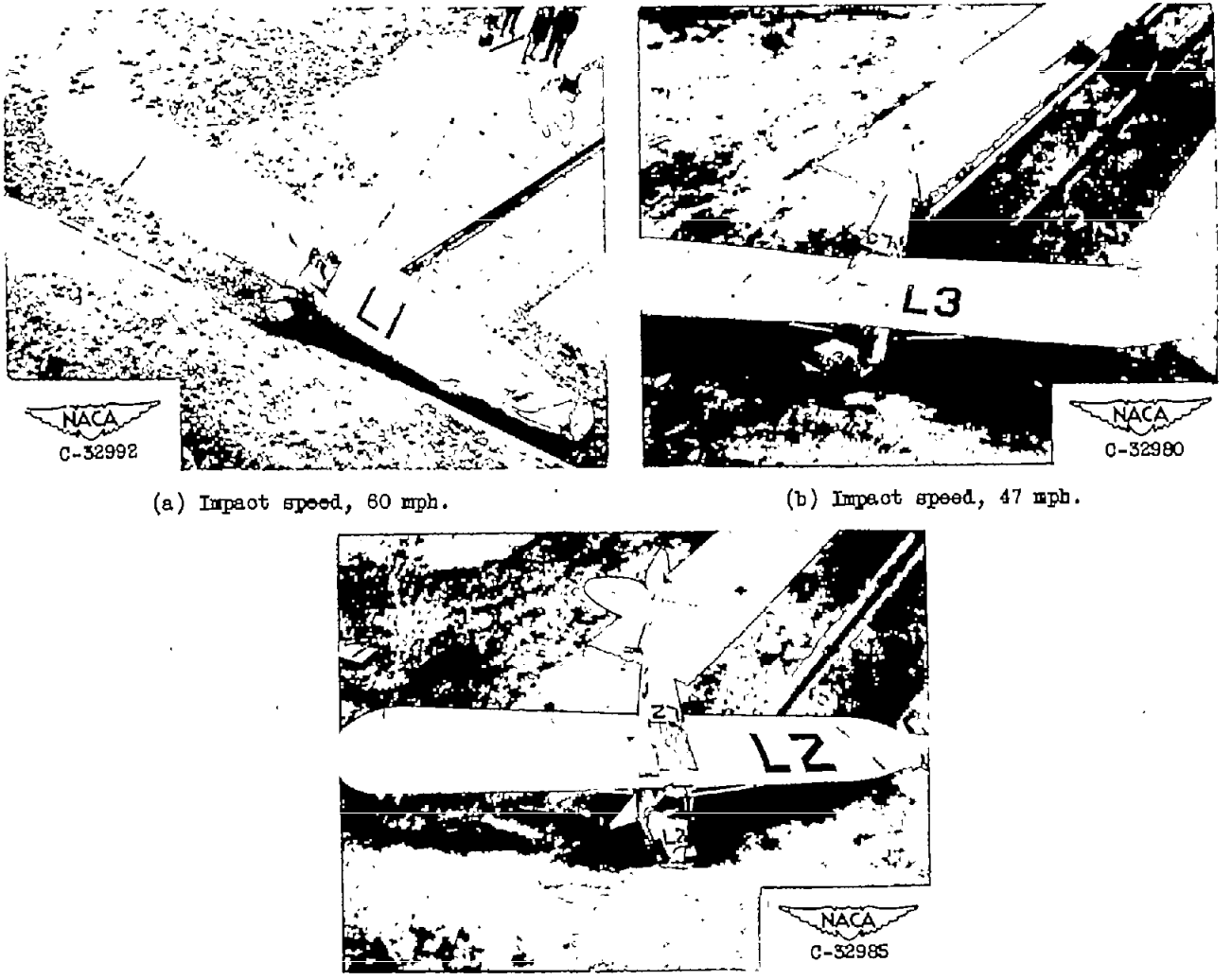

(a) Impact speed, 60 mph.

(b) Impact speed, 47 mph.

(c) Impact speed, 42 mph.

Figure 8. - Damage to wing and fuselage of airplane resulting from impact with crash barrier.

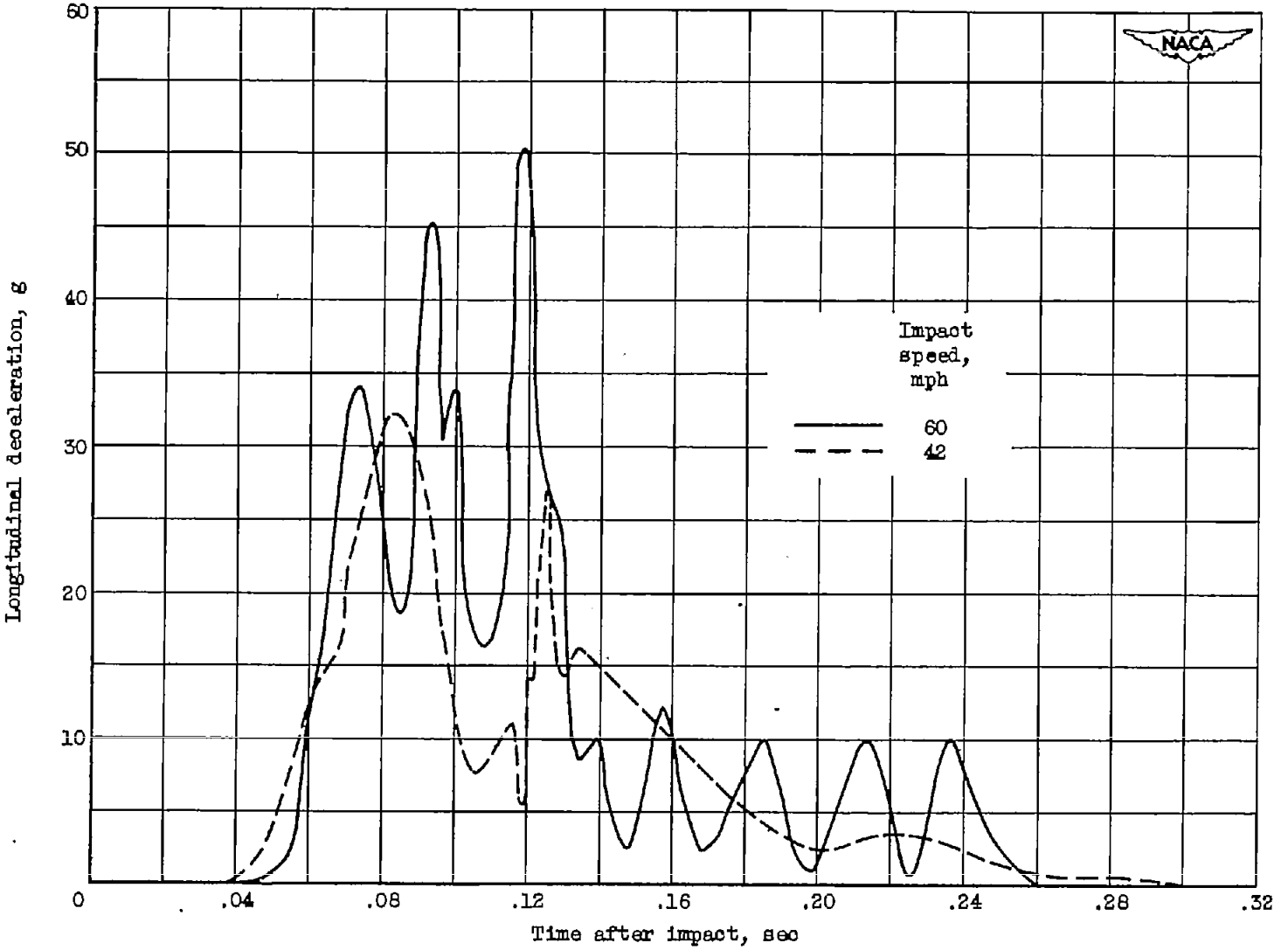

Figure 9. - Effect of impact speed on longitudinal deceleration of rear dummy's chest.

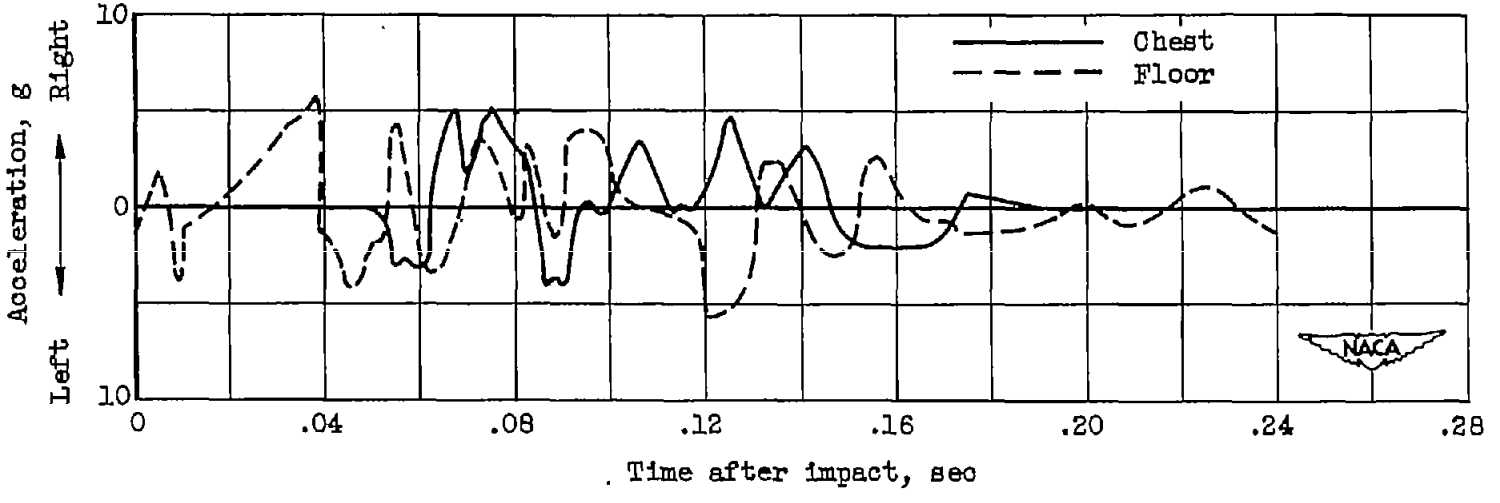

Figure 10. - Time history of lateral acceleration as measured on chest of rear dummy and fuselage floor at rear seat in 42-mph crash.

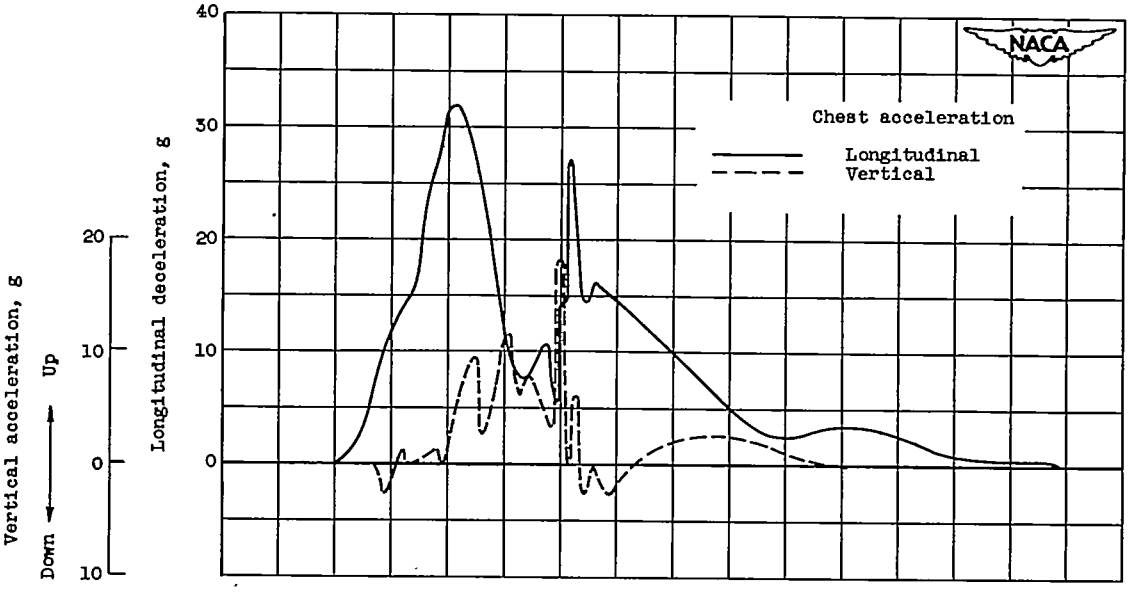

(a) Longitudinal and vertical chest accelerations. Impact speed, 42 mph.

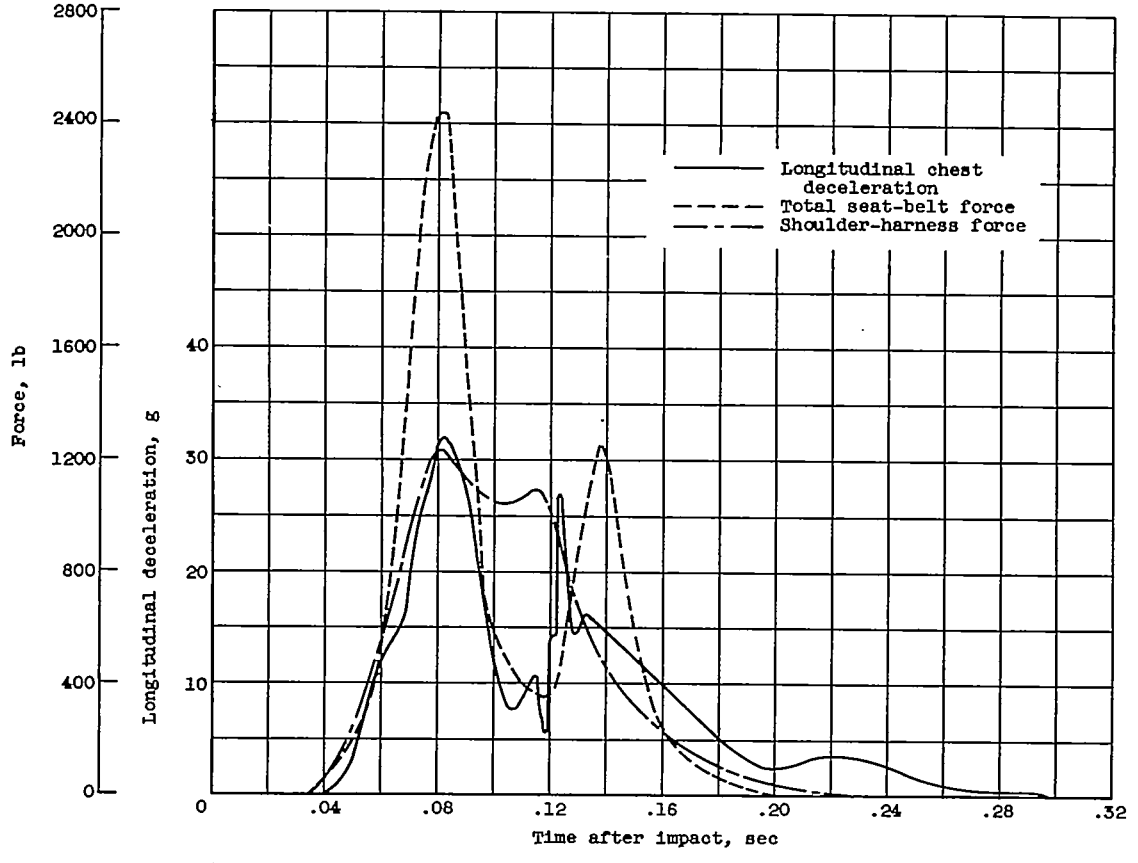

(b) Longitudinal chest deceleration and restraining forces. Impact speed, 42 mph.

Figure 11. - Relation of harness restraining forces to vertical and longitudinal chest accelerations.

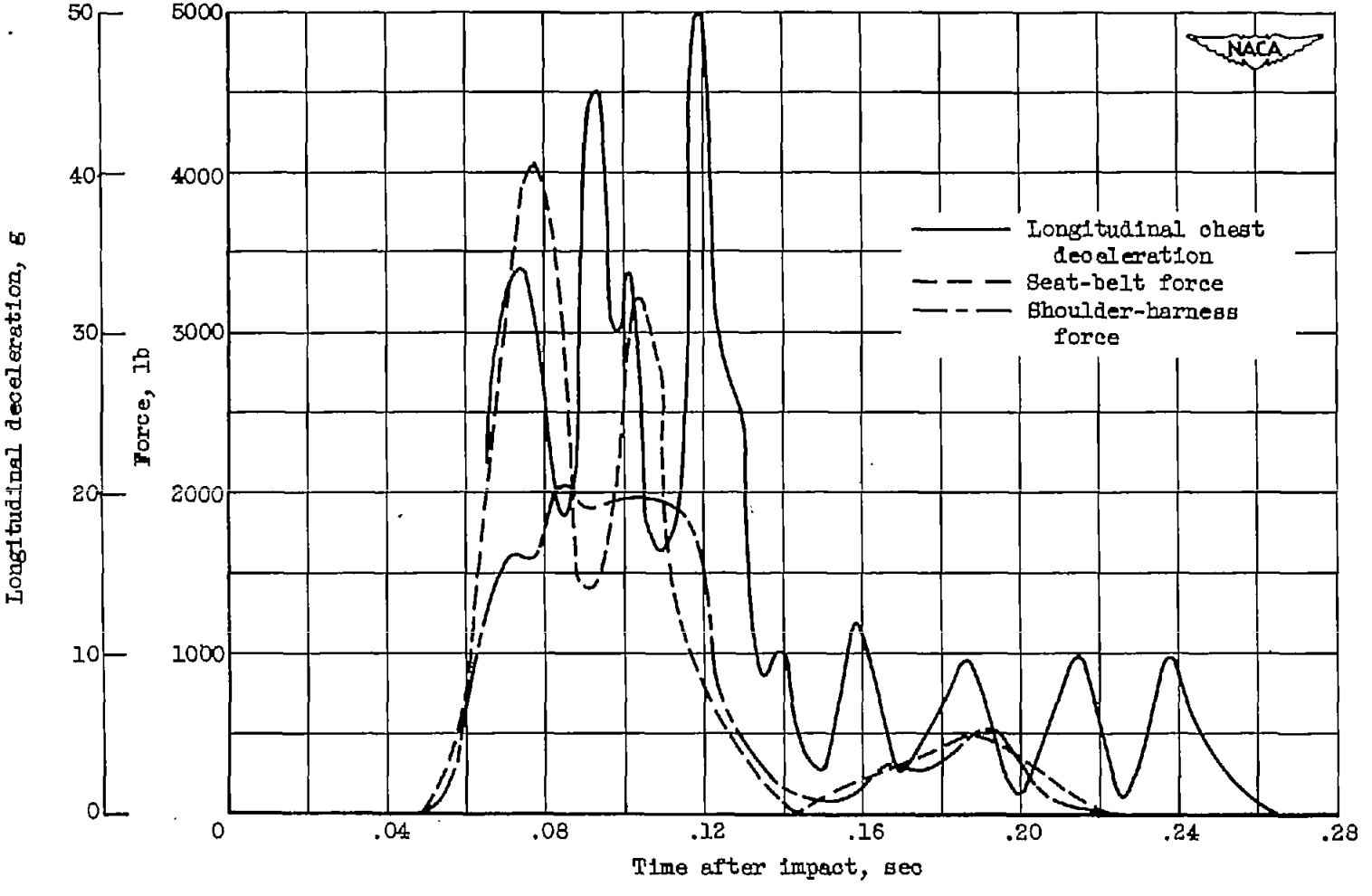

(c) Longitudinal chest deceleration and restraining forces. Impact speed, 60 mph.

Figure 11. - Concluded. Relation of harness restraining forces to vertical and longitudinal chest accelerations.

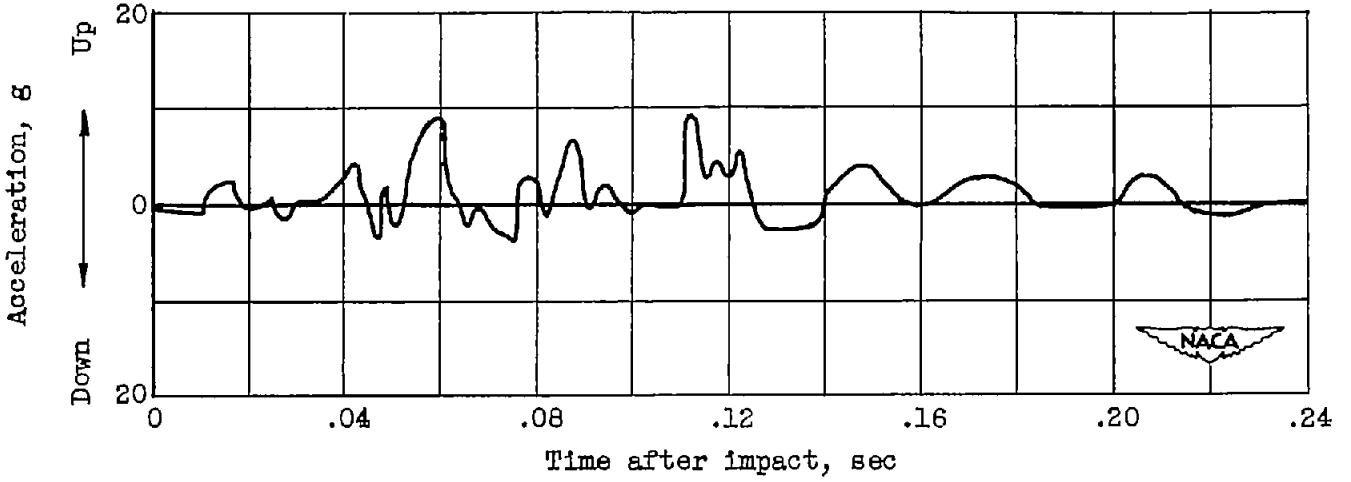

Figure 12. - Vertical acceleration of fuselage floor at rear seat in 42-mph crash.

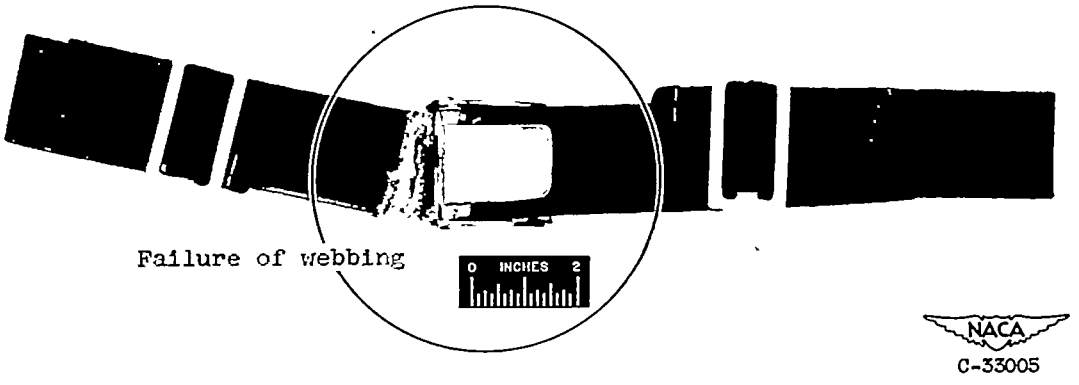

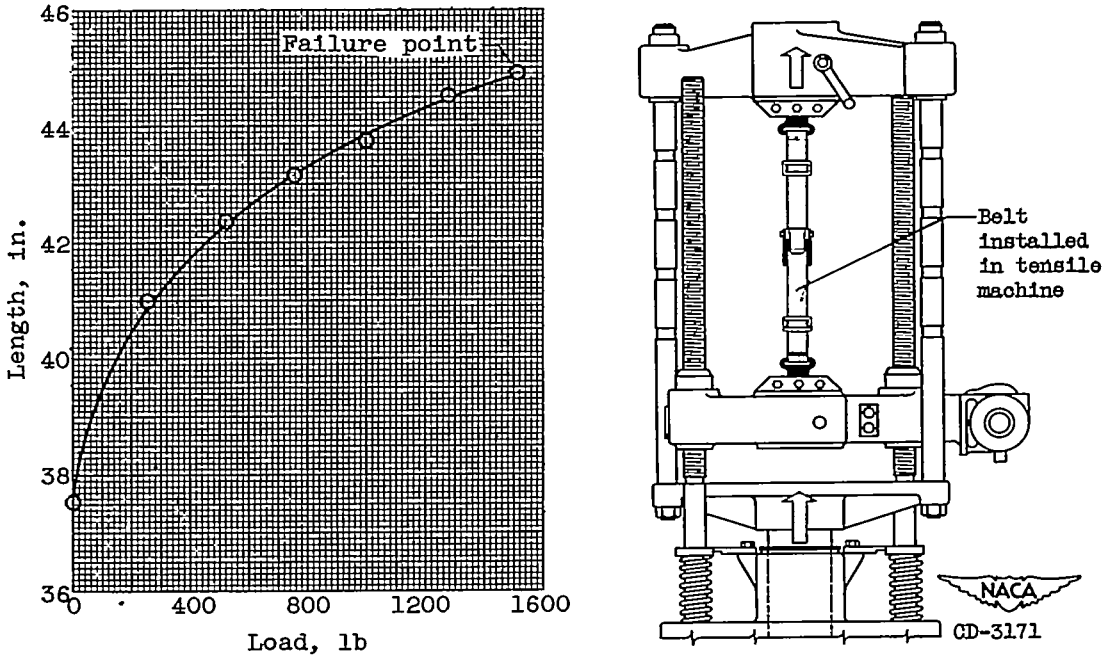

(a) Light-airplane seat belt (new). Width, 2 inches; Air Associates model number, M-5100; rated strength of assembly, 1500 pounds.

Figure 13. - Results of static tensile tests on airplane safety belts.

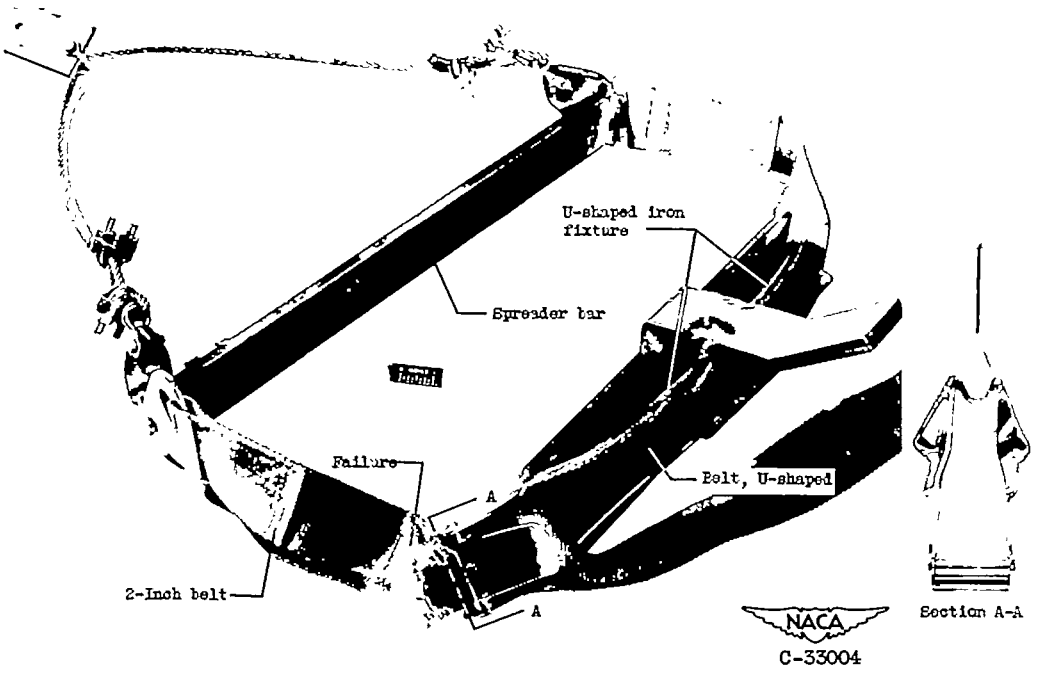

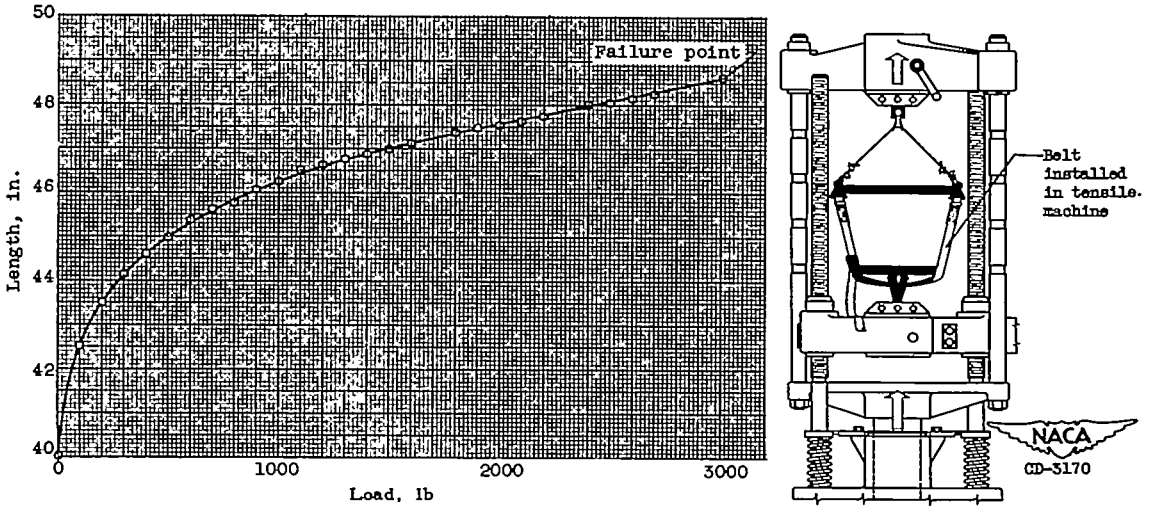

(b) Light-airplane seat belt (new). Width, 2 inches; Air Associates model number, M-5100; rated strength of assembly, 1500 pounds.

Figure 13. - Continued. Results of static tensile tests on airplane safety belts.

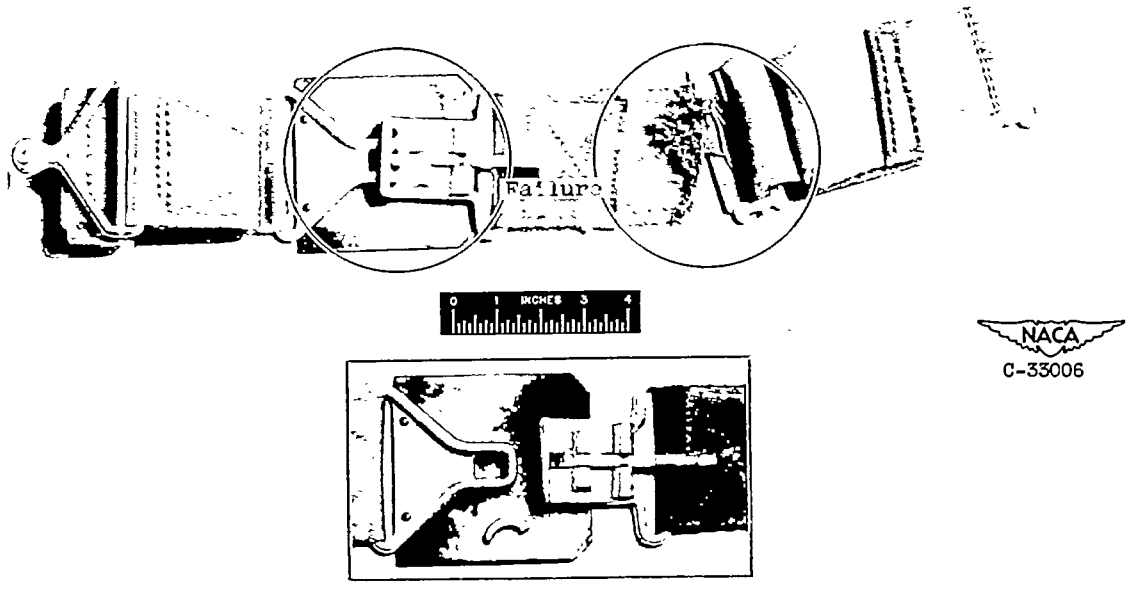

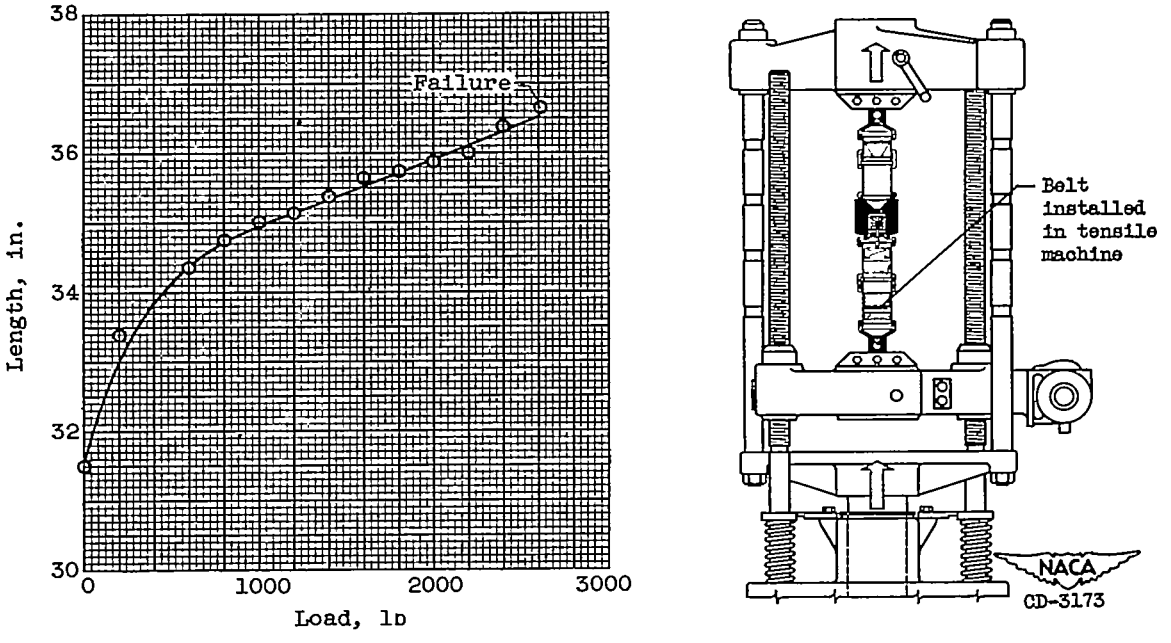

(c) Military seat belt. Width, 3 inches.

Figure 13. - Continued. Results of static tensile tests on airplane safety belts.

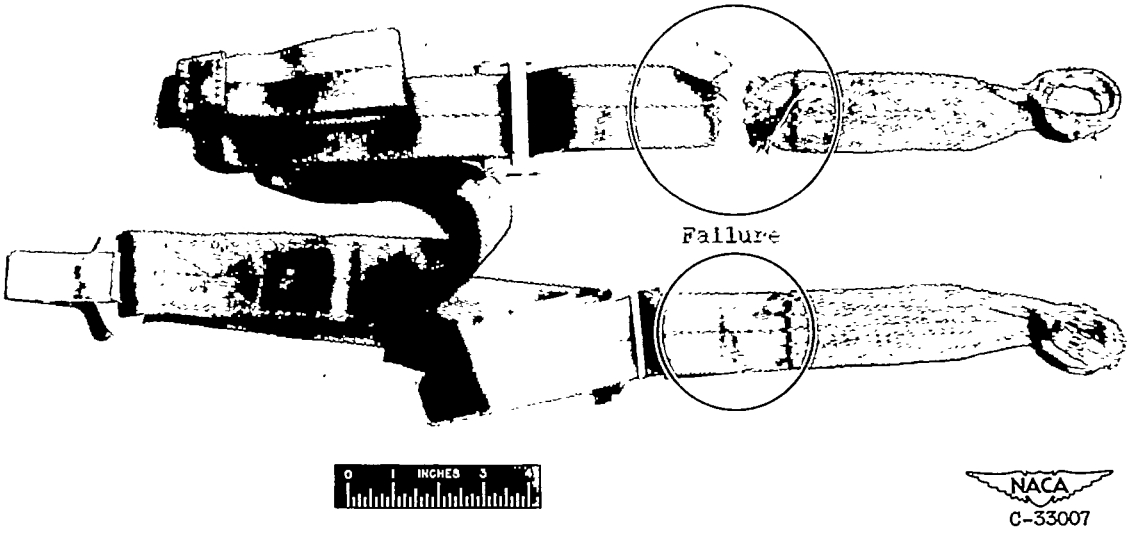

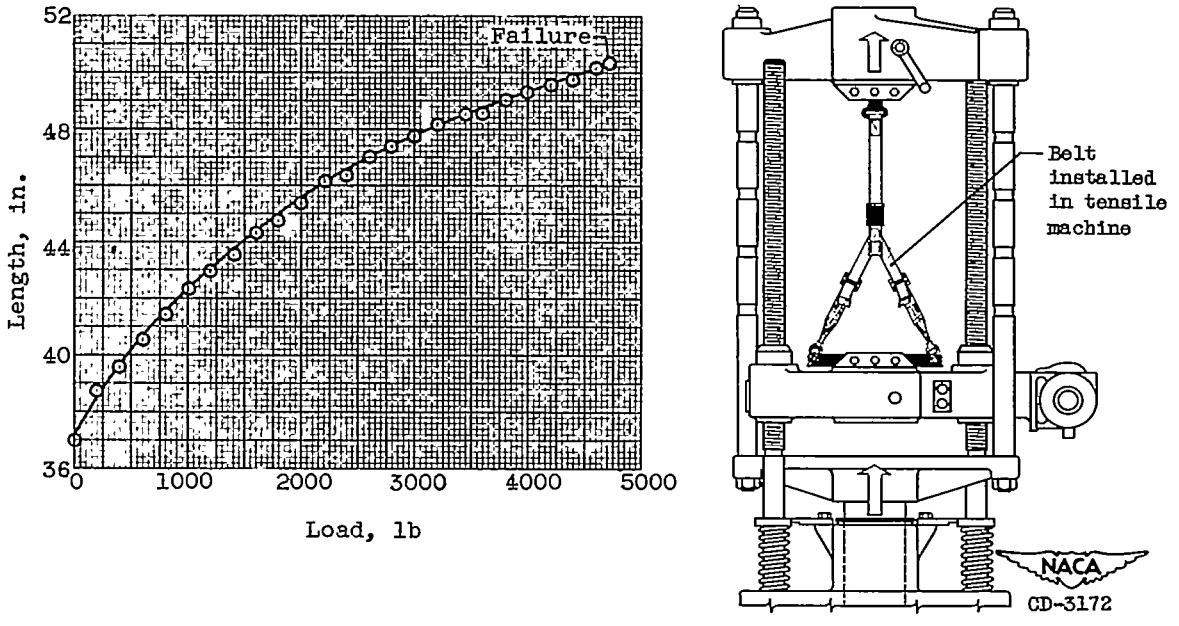

(d) Military shoulder harness. Width, $1\frac{3}{4}$ inches.

Figure 13. - Concluded. Results of static tensile tests on airplane safety belts.

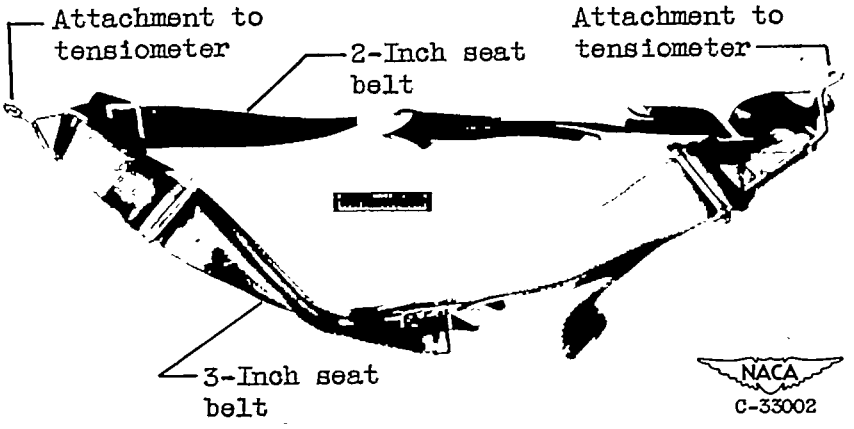

(a) Seat-belt configuration as installed on rear dummy.

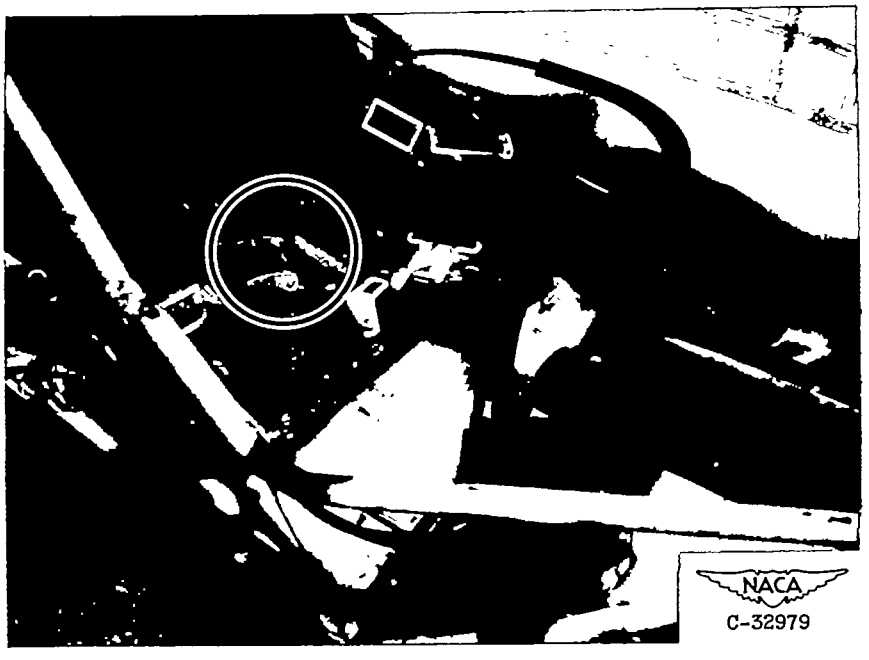

(b) Failure of 2-inch seat belt during crash.

Figure 14. - Relation of total seat-belt force to vertical and longitudinal accelerations in 47-mph crash.

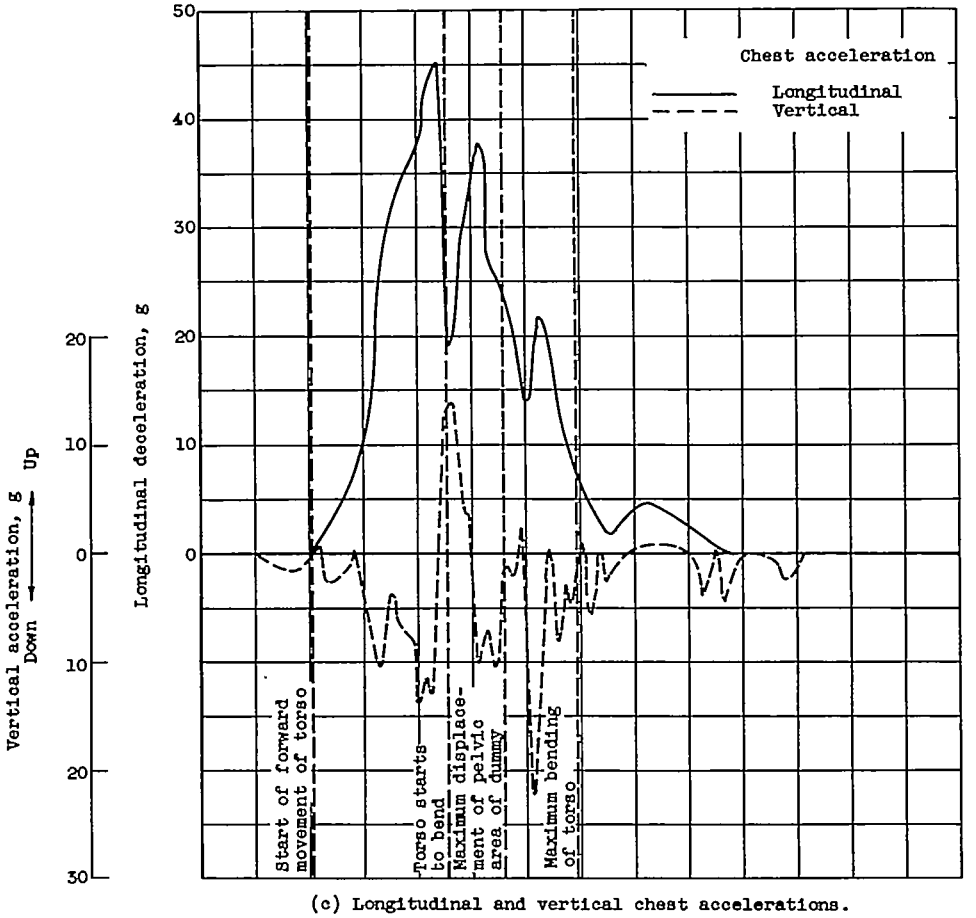

(c) Longitudinal and vertical chest accelerations.

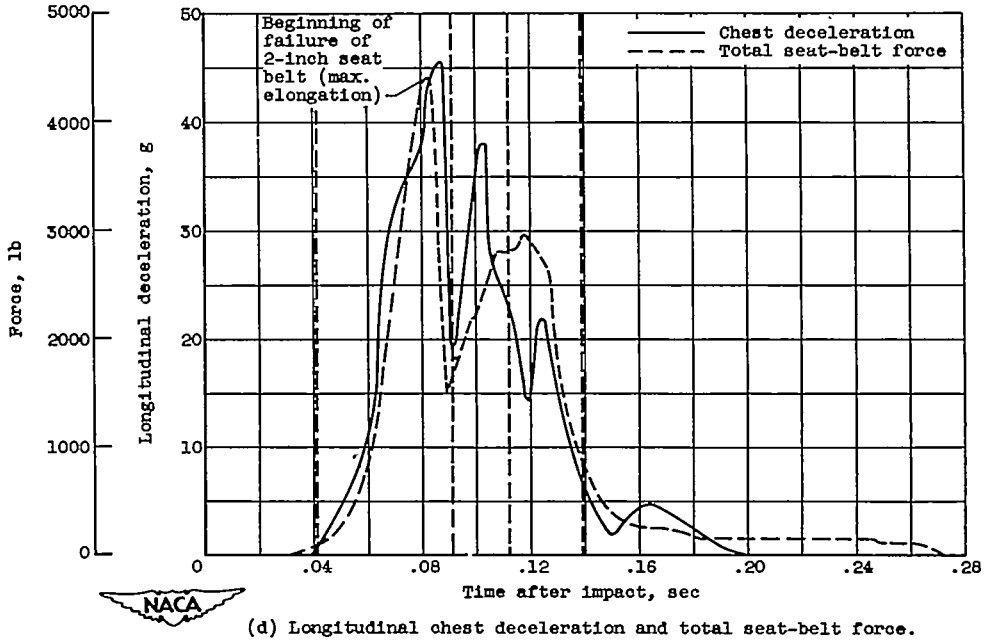

(d) Longitudinal chest deceleration and total seat-belt force.

Figure 14. - Concluded. Relation of total seat-belt force to vertical and longitudinal accelerations in 47-mph crash.

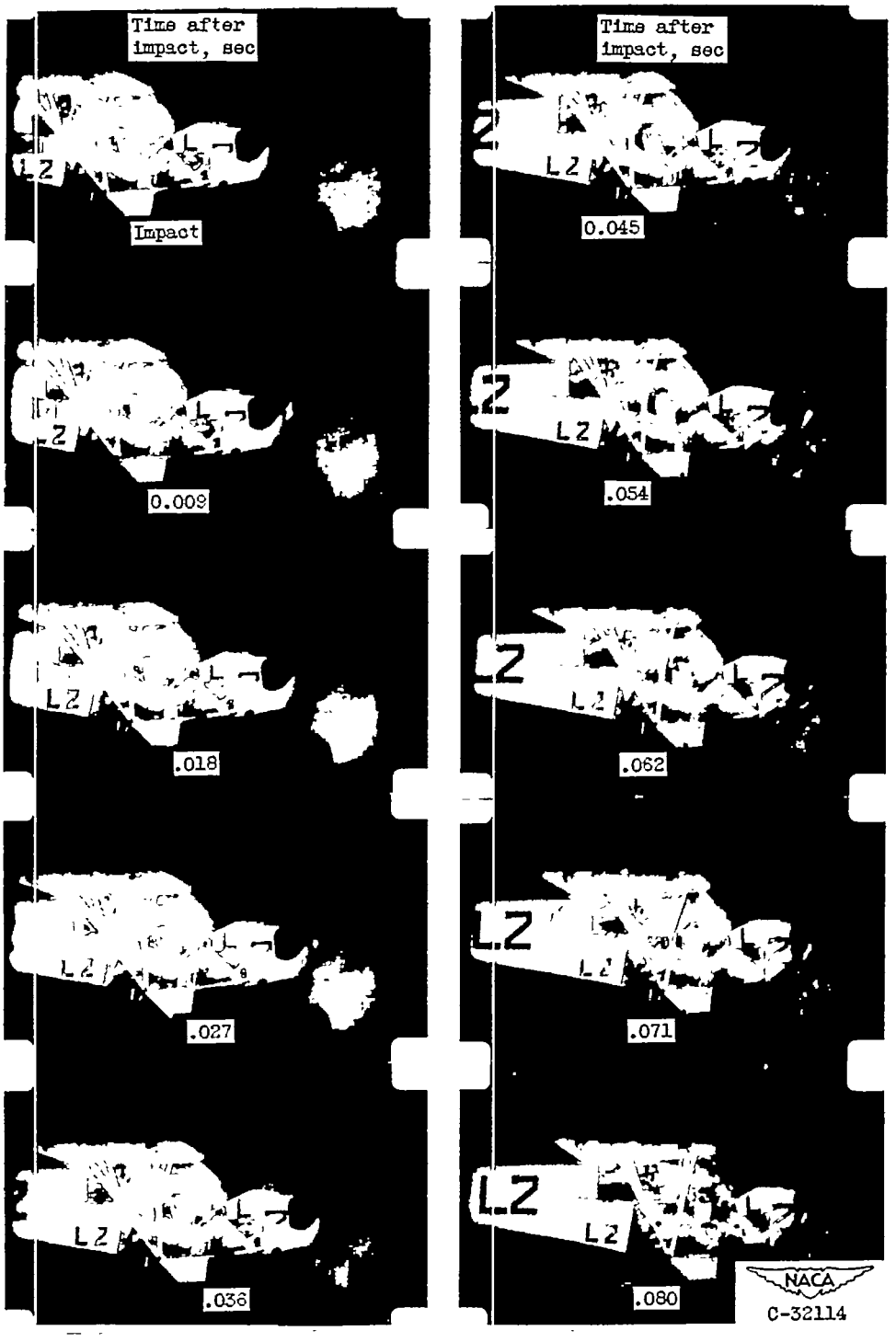

(a) Impact to 0.080 second.

Figure 15. - Displacement of airplane and dummies during deceleration in 42-mph crash.

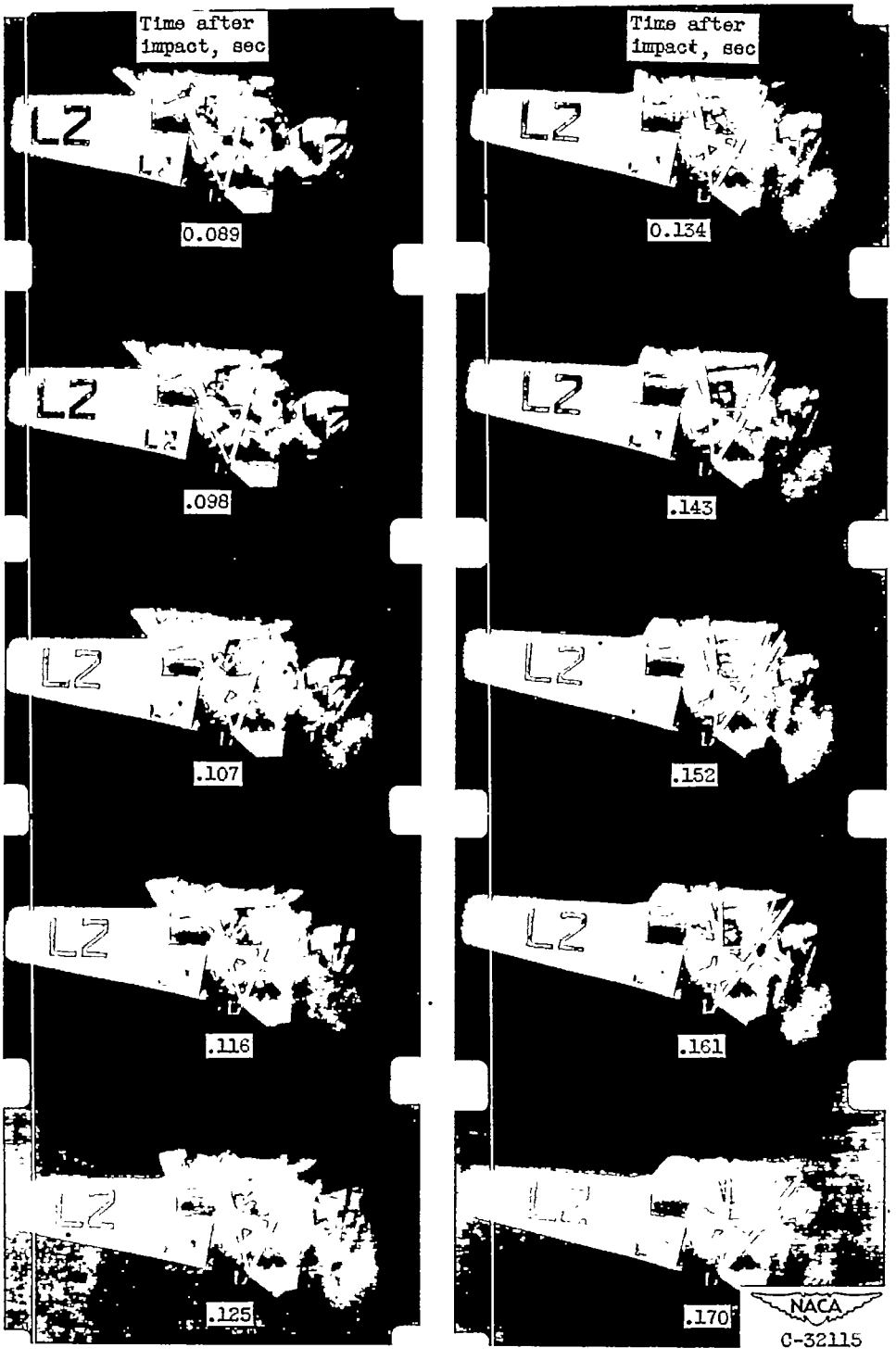

(b) 0.089 to 0.170 second.

Figure 15. - Concluded. Displacement of airplane and dummies during deceleration in 42-mph crash.

(a) Impact speed, 60 mph.

Figure 16. - Position of parachute dummy in front seat of airplane after crash.

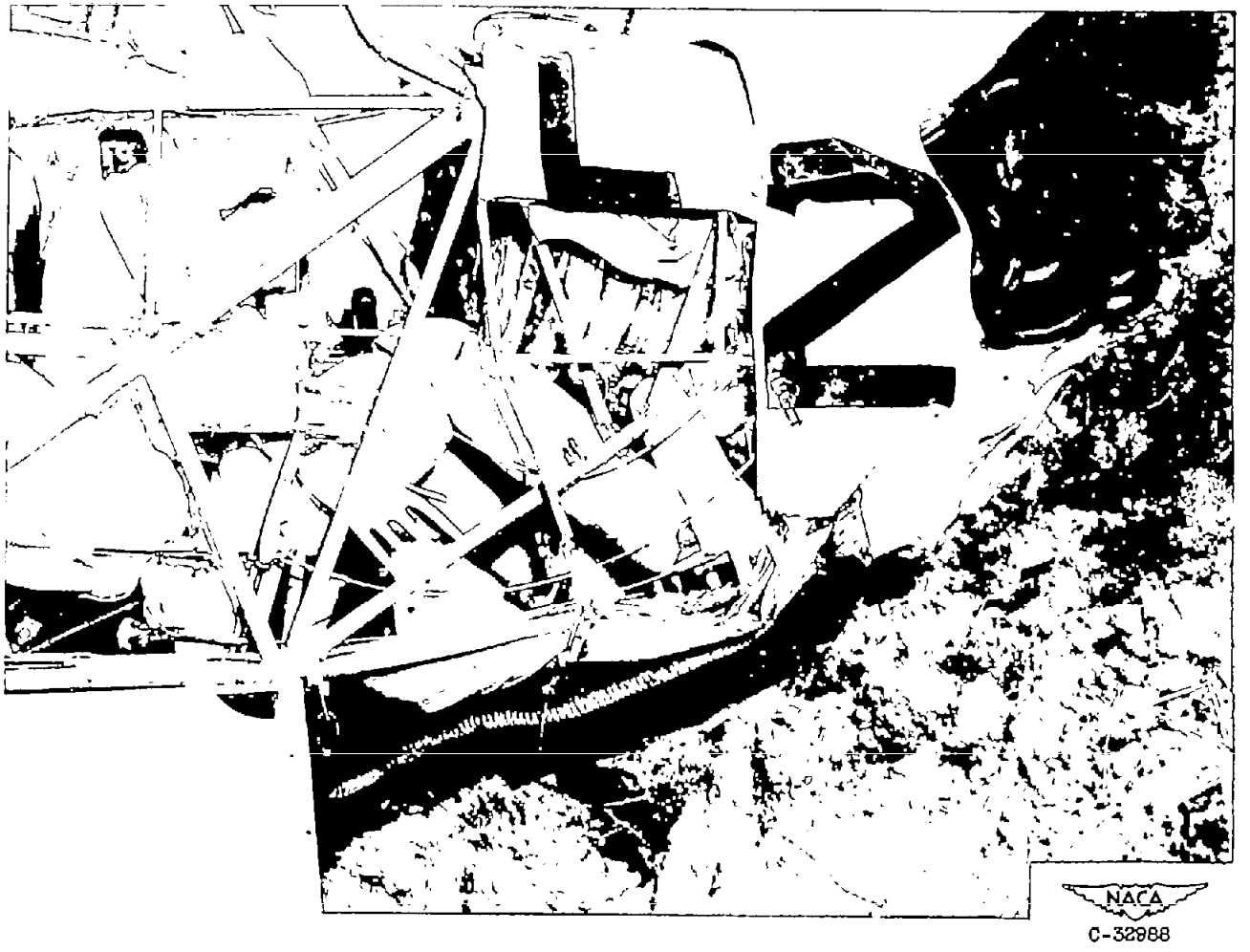

(b) Impact speed, 42 mph.

Figure 16. - Concluded. Position of parachute dummy in front seat of airplane after crash.

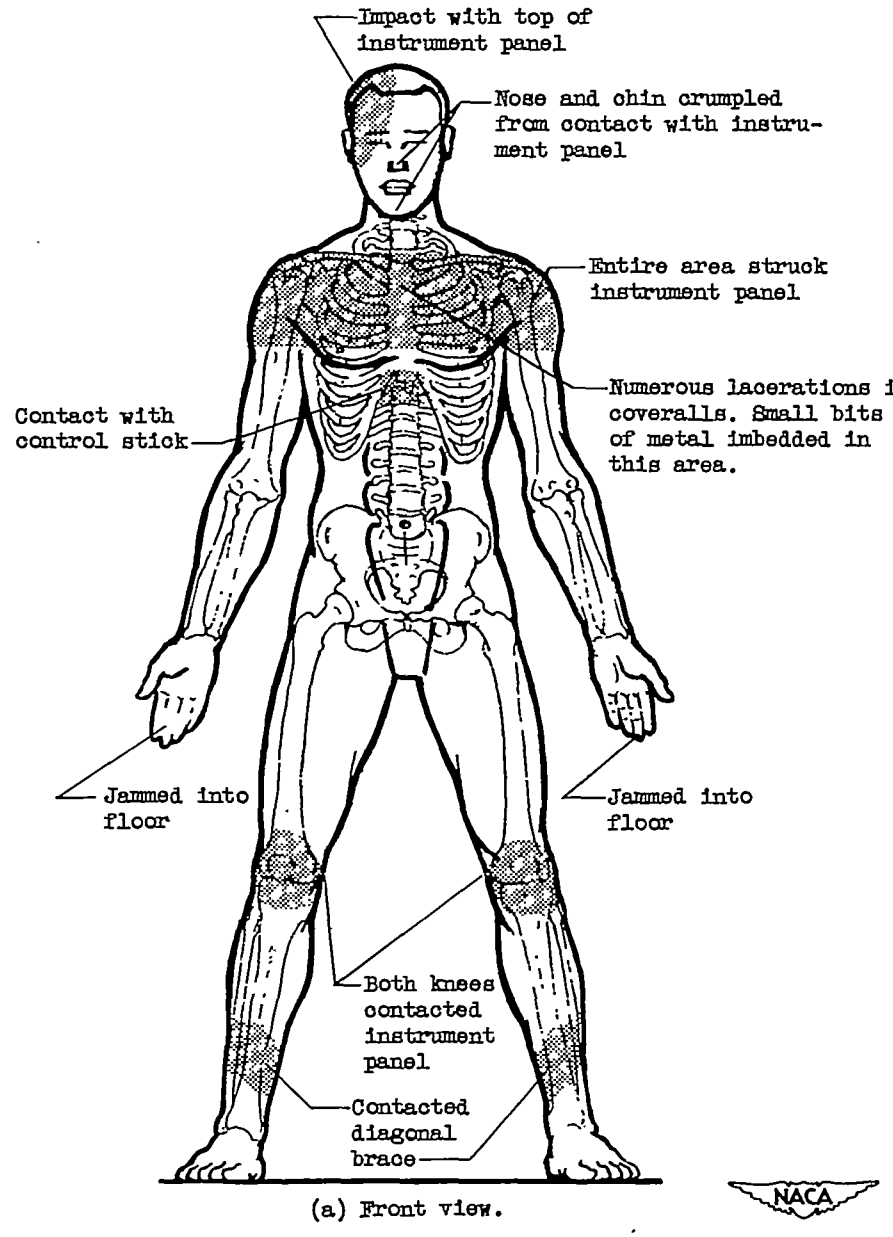

(a) Front view.

Figure 17. - Location, area, and cause of blows sustained by front-seat dummy in 60-mph crash.

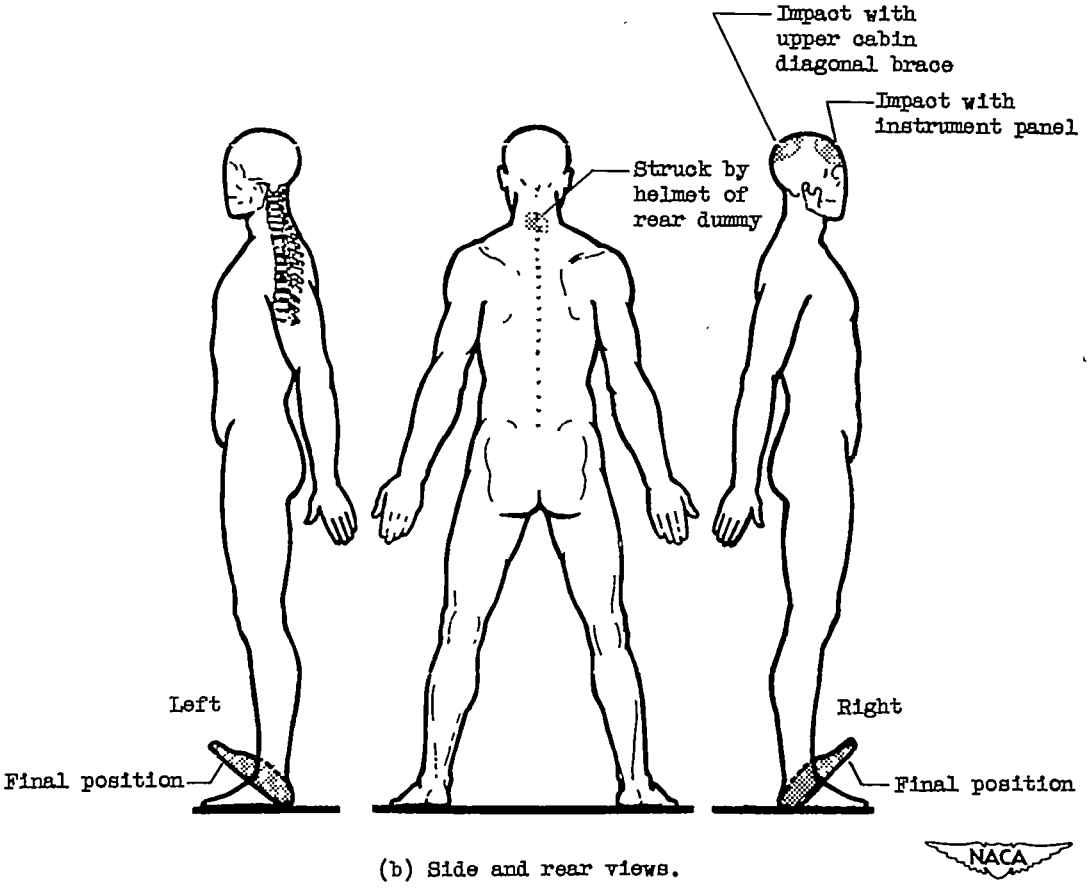

(b) Side and rear views.

Figure 17. - Concluded. Location, area, and cause of blows sustained by front-seat dummy in 60-mph crash.

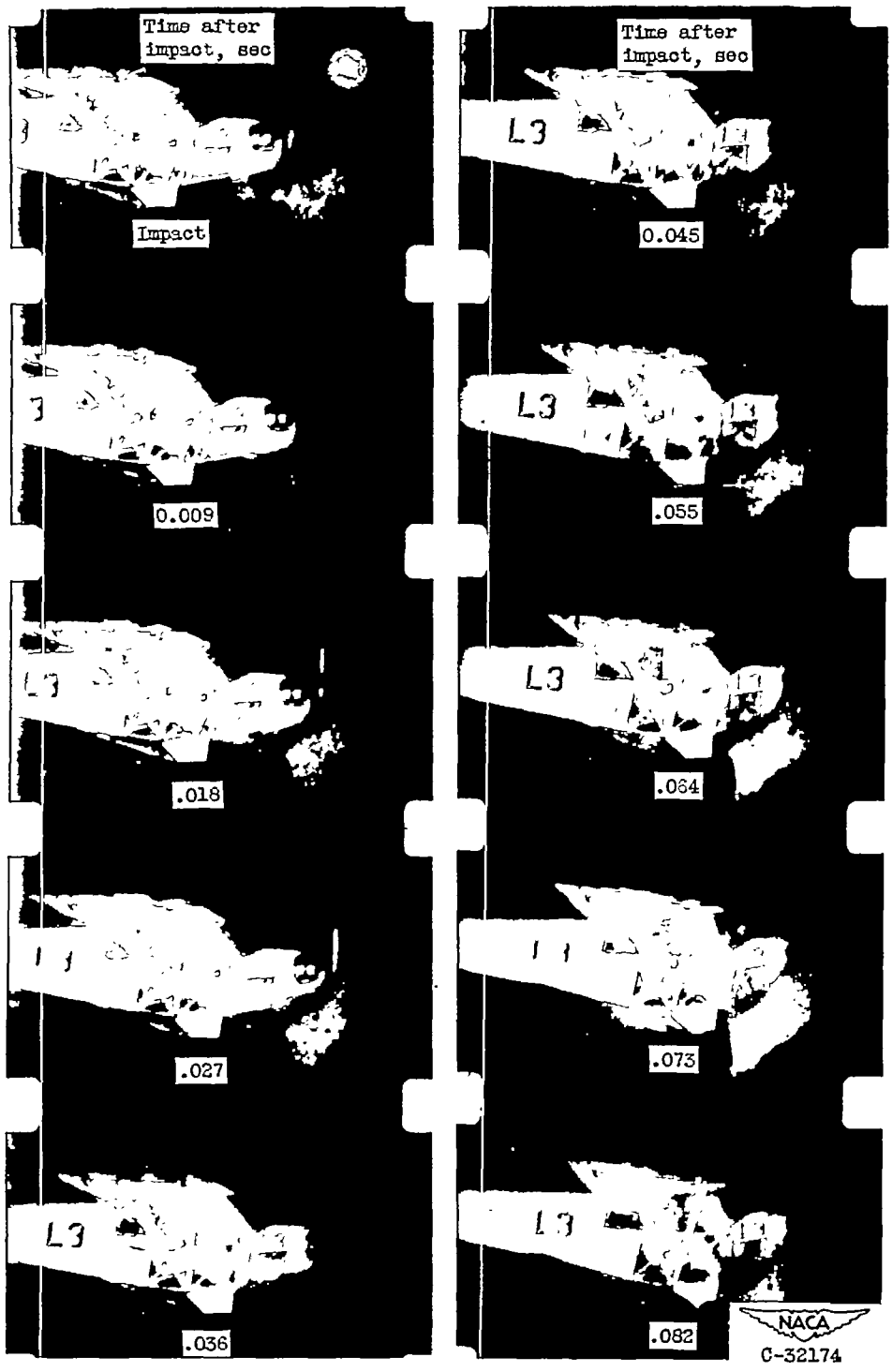

(a) Impact to 0.082 second.

Figure 18. - Displacement of airplane and rear dummy during deceleration in 47-mph crash.

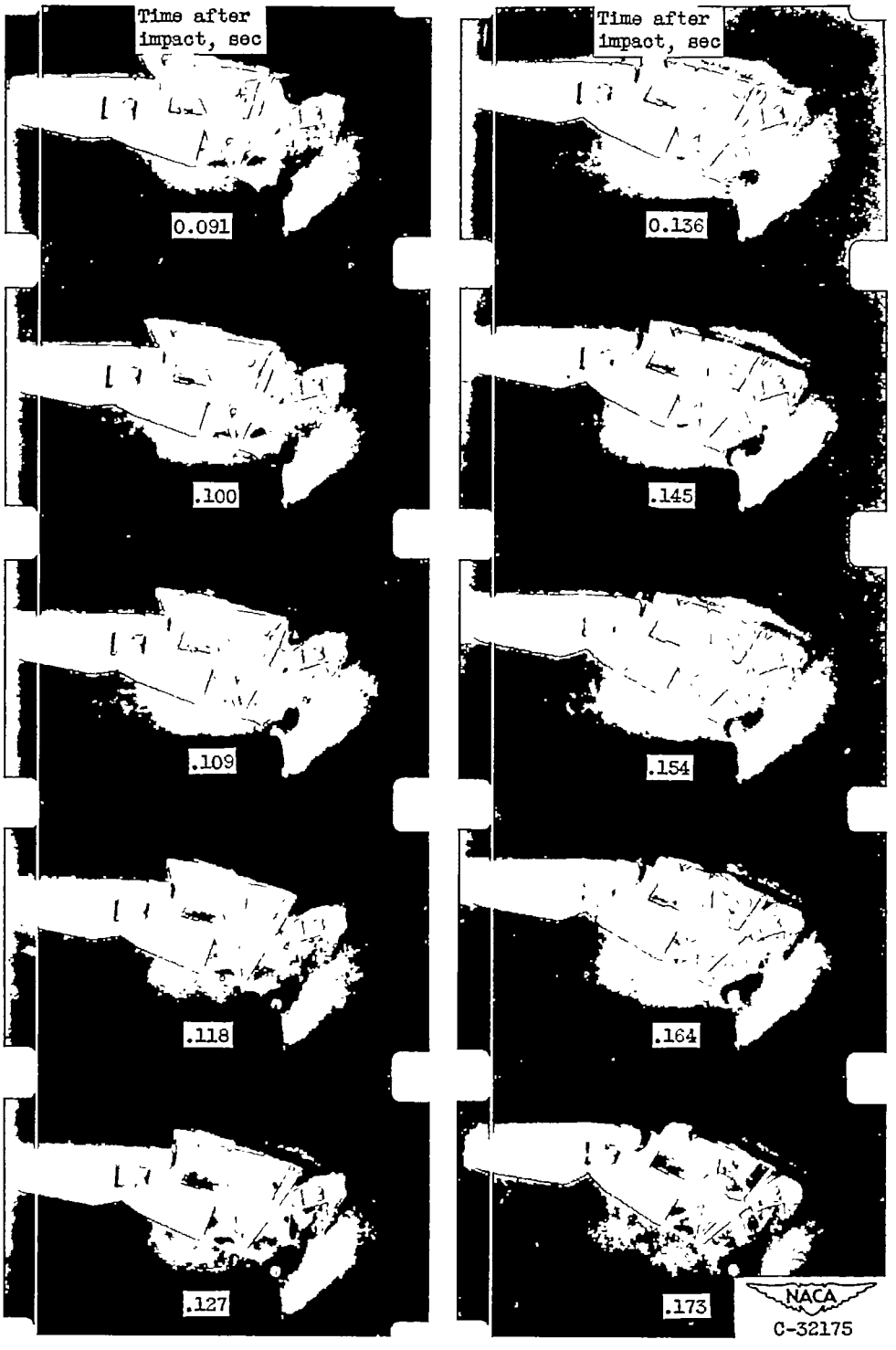

(b) 0.091 to 0.173 second.

Figure 18. - Concluded. Displacement of airplane and rear dummy during deceleration in 47-mph crash.

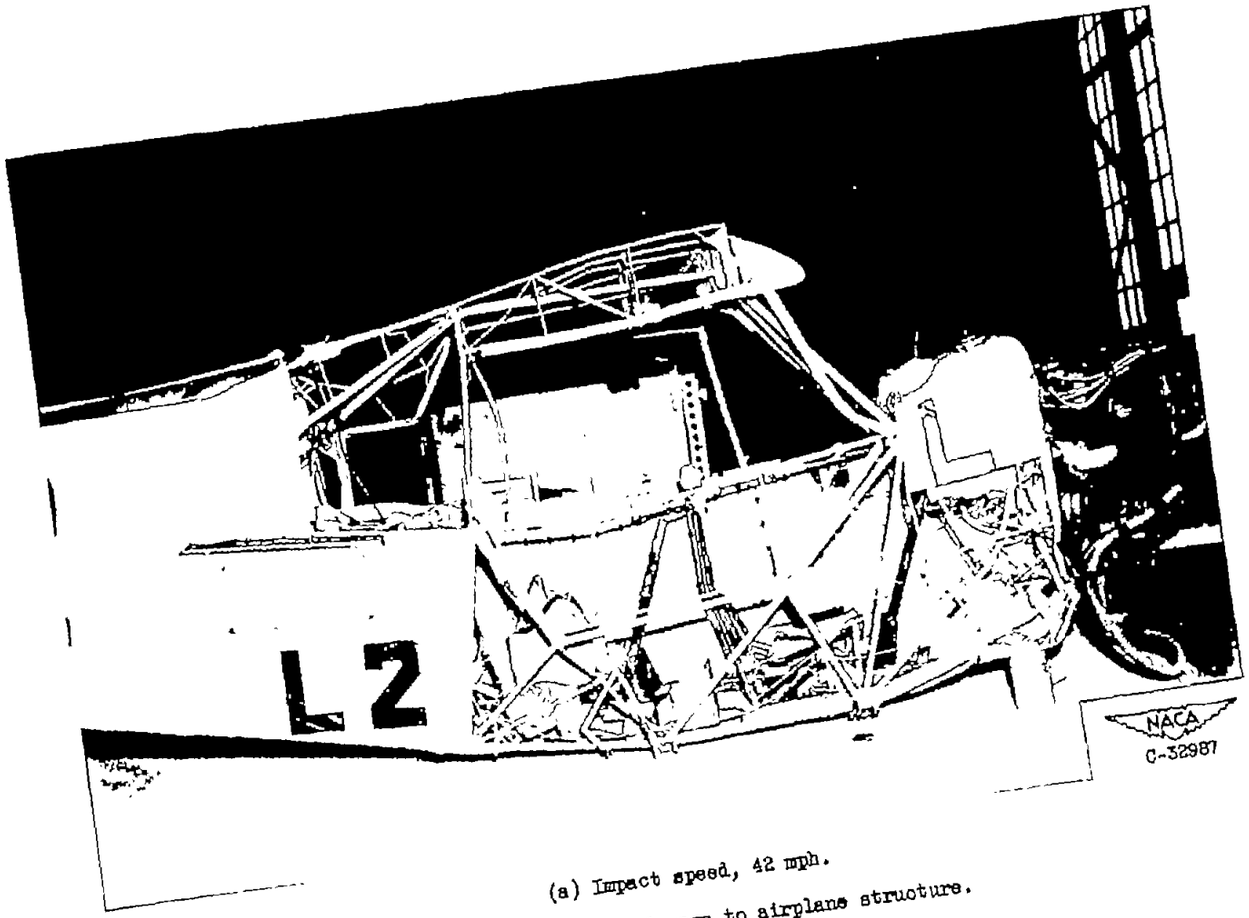

(a) Impact speed, 42 mph.

Figure 18. - Crash damage to airplane structure.

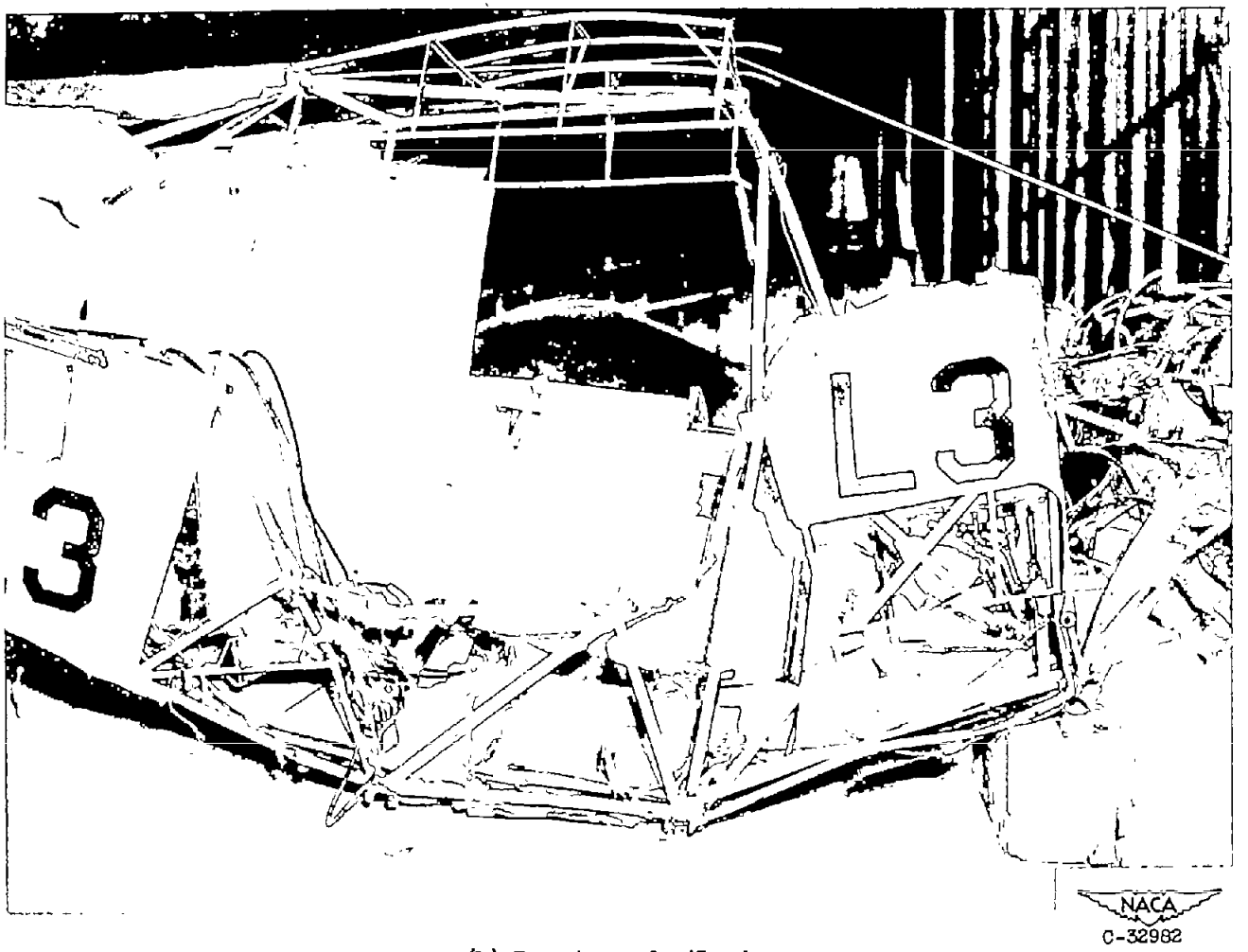

(b) Impact speed, 47 mph.

Figure 19. - Continued. Crash damage to airplane structure.

(c) Impact speed, 60 mph.

Figure 19. - Concluded. Crash damage to airplane structure.

(a) Impact speed, 60 mph.

Figure 20. - Extent of damage to full fuel tank during a crash.

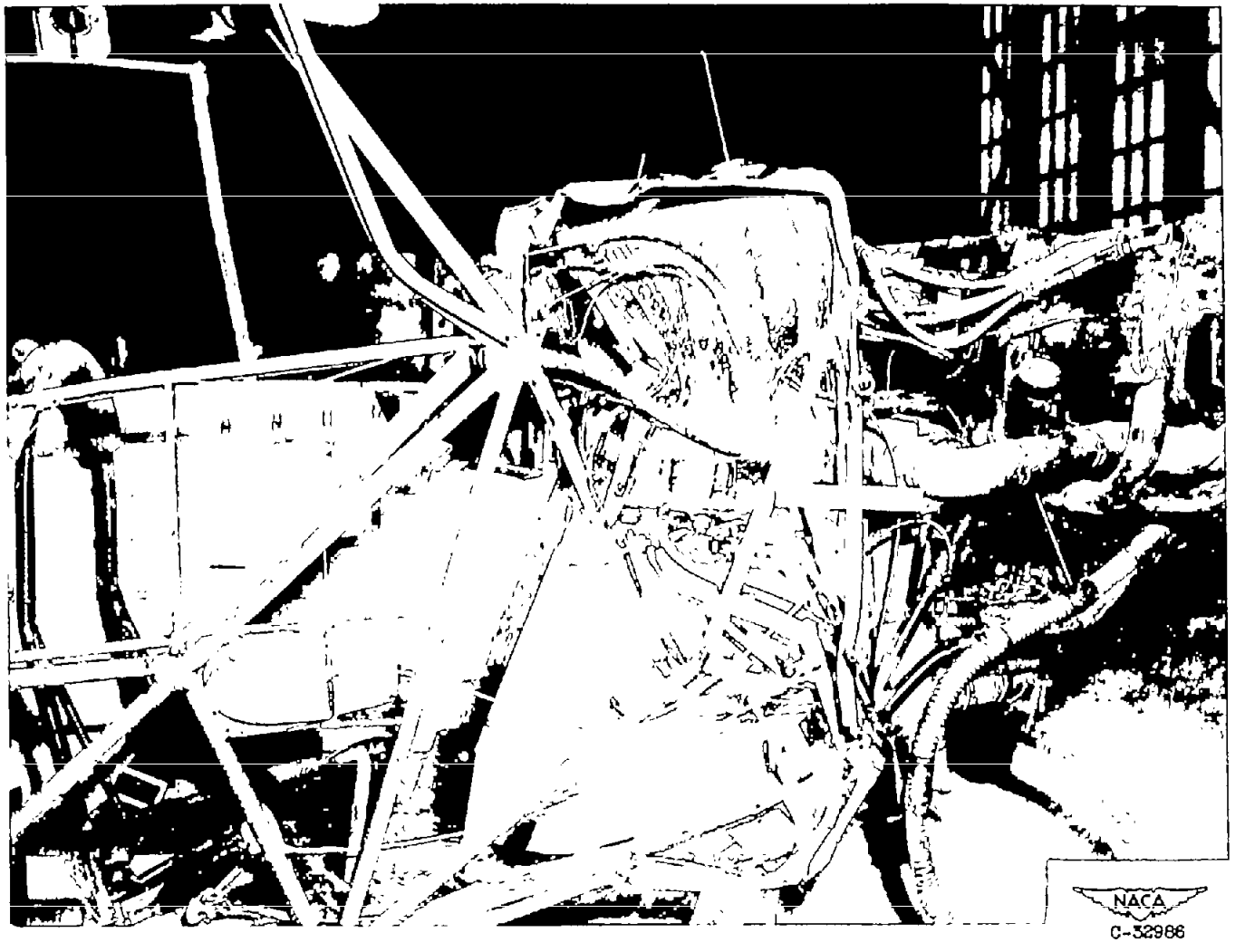

(b) Impact speed, 42 mph.

Figure 20. - Concluded. Extent of damage to empty fuel tank during a crash.

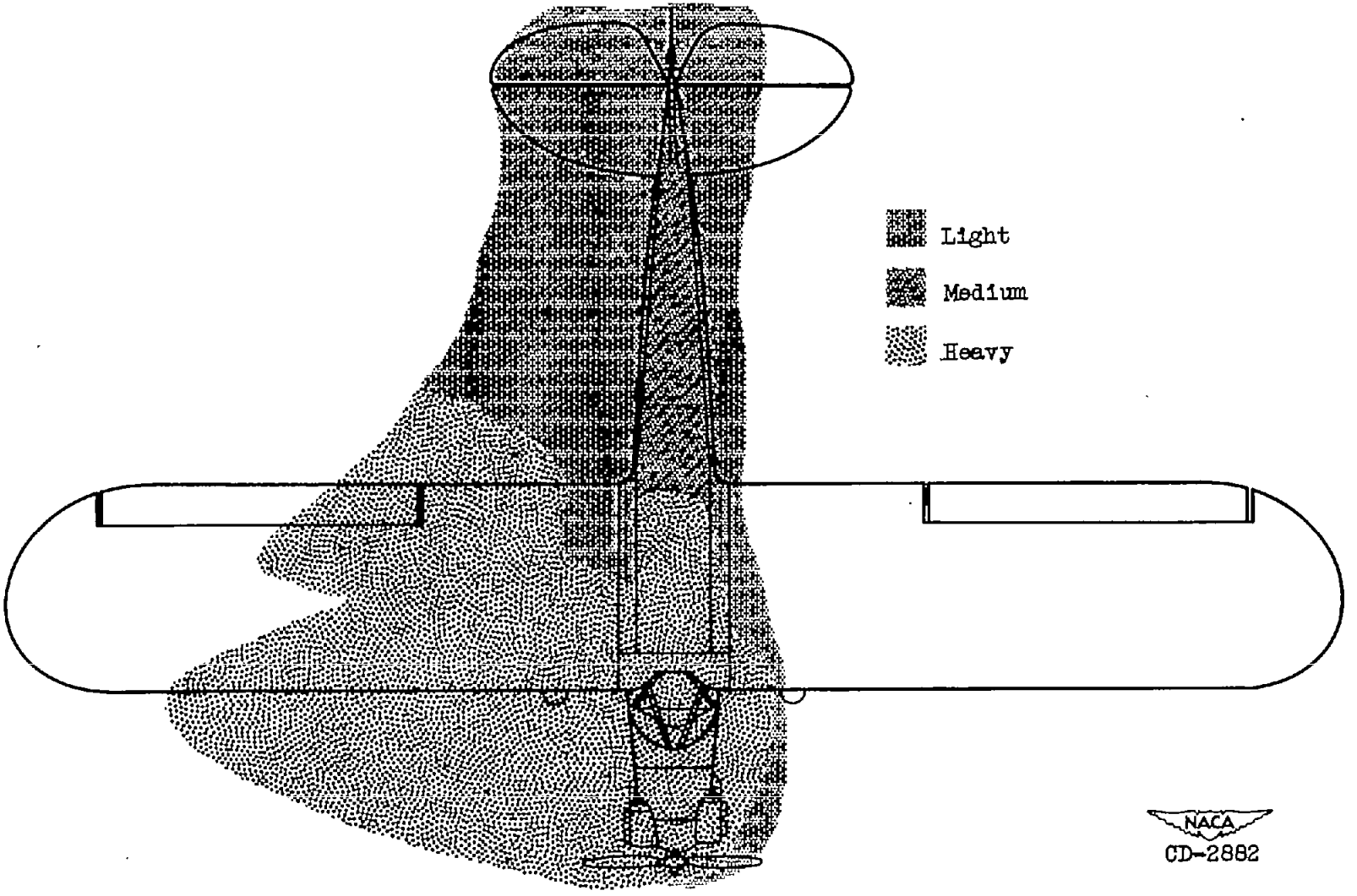

Figure 21. - Fuel-spread pattern and concentration during 60-mph crash.